



HAL
open science

Theoretical analysis of the electrochemical systems used for the application of direct current/voltage stimuli on cell cultures

Simon Guette-Marquet, Christine Roques, Alain Bergel

► **To cite this version:**

Simon Guette-Marquet, Christine Roques, Alain Bergel. Theoretical analysis of the electrochemical systems used for the application of direct current/voltage stimuli on cell cultures. *Bioelectrochemistry*, 2021, 139, pp.107737. 10.1016/j.bioelechem.2020.107737 . hal-03136237

HAL Id: hal-03136237

<https://hal.science/hal-03136237>

Submitted on 9 Feb 2021

HAL is a multi-disciplinary open access archive for the deposit and dissemination of scientific research documents, whether they are published or not. The documents may come from teaching and research institutions in France or abroad, or from public or private research centers.

L'archive ouverte pluridisciplinaire **HAL**, est destinée au dépôt et à la diffusion de documents scientifiques de niveau recherche, publiés ou non, émanant des établissements d'enseignement et de recherche français ou étrangers, des laboratoires publics ou privés.



Open Archive Toulouse Archive Ouverte

OATAO is an open access repository that collects the work of Toulouse researchers and makes it freely available over the web where possible

This is an author's version published in: <http://oatao.univ-toulouse.fr/27404>

Official URL : <https://doi.org/10.1016/j.bioelechem.2020.107737>

To cite this version:

Guette-Marquet, Simon  and Roques, Christine  and Bergel, Alain 
Theoretical analysis of the electrochemical systems used for the application of direct current/voltage stimuli on cell cultures. (2021) *Bioelectrochemistry*, 139. ISSN 1567-5394

Any correspondence concerning this service should be sent to the repository administrator: tech-oatao@listes-diff.inp-toulouse.fr

Theoretical analysis of the electrochemical systems used for the application of direct current/voltage stimuli on cell cultures

Simon Guette-Marquet, Christine Roques, Alain Bergel*

Laboratoire de Génie Chimique, Université de Toulouse, CNRS, INPT, UPS, Toulouse, France

ARTICLE INFO

Article history:

Received 16 June 2020

Received in revised form 22 December 2020

Accepted 29 December 2020

Available online 4 January 2021

Keywords:

Electric field

Conductive polymer

Electrotaxis

Galvanotaxis

Tissue engineering

Stem cell

ABSTRACT

Endogenous electric fields drive many essential functions relating to cell proliferation, motion, differentiation and tissue development. They are usually mimicked *in vitro* by using electrochemical systems to apply direct current or voltage stimuli to cell cultures. The many studies devoted to this topic have given rise to a wide variety of experimental systems, whose results are often difficult to compare. Here, these systems are analysed from an electrochemical standpoint to help harmonize protocols and facilitate optimal understanding of the data produced.

The theoretical analysis of single-electrode systems shows the necessity of measuring the Nernst potential of the electrode and of discussing the results on this basis rather than using the value of the potential gradient. The paper then emphasizes the great complexity that can arise when high cell voltage is applied to a single electrode, because of the possible occurrence of anode and cathode sites. An analysis of two-electrode systems leads to the advice to change experimental practices by applying current instead of voltage. It also suggests that the values of electric fields reported so far may have been considerably overestimated in macro-sized devices. It would consequently be wise to revisit this area by testing considerably lower electric field values.

1. Introduction

The role of electric stimuli in the development of living tissues has been hypothesized for a very long time [1]. Marsh and Beams even noted that speculations on the intervention of endogenous “electrical forces” in the development of the nervous system of vertebrates dated back to the 19th century [2]. In 1964, Bassett et al. started their article devoted to the effect of electric field on bones by the sentence: “*It now seems evident that bone functions as a transducer, converting mechanical energy to electrical energy*” [3]. Nevertheless, in spite of researchers’ longstanding interest in the influence of electrical fields on cell growth and organism development, the mechanisms remain poorly understood, and it was still possible to write in 2018: “*cell response to electrical stimuli is a mystery*” [4].

As reviewed recently [5,6], endogenous electric fields are now known to play many essential roles in living organisms, not just for the transmission of nerve impulses or muscle contraction but also in controlling cell morphology, gene expression, and cell proliferation and migration, including some impacts on tumour

growth [7,8]. Electric gradients of 15–60 mV, the so-called *trans-epithelial potential* (TEP), have typically been observed in skin, lens and cornea [9–14]. In a vertebrate lens, TEP creates current loops with magnitudes around 20–40 mA/cm², which guide the migration and affect the differentiation of epithelial cells [9,15]. TEP has been found to be a major motor of wound healing [13,14] by directing cell migration toward the injury [14,16,17] and also controlling the orientation and frequency of cell division [10].

Experiments performed on aquatic worms [18] and frogs [19] showed that so-called “membrane voltage-dependent bioelectric signalling” was a key parameter in the formation and location of organs [18,20]. The concept of “bioelectric code” has thus been launched [21] as a possible explanation for pattern regulation in living organisms.

The use of external electrical stimulation is now well-established in medicine [5]. Electrical stimulation is largely used to fix bone defects and repair fractures by promoting osteogenesis [22–23]. It has also been successfully tested on small animals to heal complex wounds [24]. Electric stimulation is also envisioned as a way to control the proliferation, differentiation and spatial location of stem cells [25–28].

The great majority of the studies devoted to electric stimuli use transient stimuli, which can be monophasic or biphasic and applied in various forms, such as sinusoids, square waves or pulses,

* Corresponding author at: Laboratoire de Génie Chimique, 4 allée Emile Monso, 31432 Toulouse, France.

E-mail address: alain.bergel@toulouse-inp.fr (A. Bergel).

with frequencies generally ranging from a few Hz to 100 Hz [5]. The present article does not address such transient stimuli and focuses only on direct ones. Direct current or voltage stimuli can be considered to mimic the electrical conditions that occur in living organisms and thus constitute a tool that can make a great contribution to progress in deciphering the functions and mechanisms of endogenous electrical phenomena.

Direct electrical stimuli are often named direct current (DC) stimuli in the literature. We avoid this term here because, in some cases, only a potential gradient is applied without any current flowing through the system. The term “direct electrical stimuli (DES)” is consequently preferred and will be used hereafter.

Even on the limited area of DES, a significant variety of signals and experimental devices are found in the literature. DES can be applied by controlling a variety of parameters: current (A), current density ($A.m^{-2}$), potential difference between two electrodes (V) or electric field ($V.m^{-1}$). The experimental details required to extract the values of all these parameters from each study are not always available, which often hinders direct comparison of the data produced by different research groups.

The experimental devices, which are most often lab made, also present a large variety of configurations. Some of these systems are not commonly used in the field of conventional electrochemistry. Here, it was decided to organize the theoretical analysis of these experimental devices in four sections according to the number of electrodes the system is equipped with: zero, one, two or three.

The present work intends to afford a rigorous theoretical analysis of the devices used to apply DES, from the standpoint of electrochemistry. We hope that such electrochemical basics will help to facilitate further comparisons of experimental reports and to optimize the experimental devices and procedures. *In vitro* DES application opens up promising avenues towards an understanding of the roles of endogenous electrical phenomena. This article hopes to provide the multi-disciplinary research community engaged on this path with a rigorous electrochemical contribution.

2. Materials and methods

Experiments were performed in NaCl–phosphate buffer solution pH 7.0–7.3 (Gibco DPBS 1X). The graphite electrode was a $2.5 \times 2.5 \text{ cm}^2$ foil, 0.3 cm thick (Goodfellow C 000330) connected electrically by two platinum wires (0.5 mm in diameter). The Pt wires were below the graphite electrode, in contact with it over a length of 2 cm, and 1.7 cm apart. The wires and the electrode were held firmly against each other between two Teflon plates that were screwed together. A circular hole of 11 mm diameter in the upper Teflon plate determined the volume of the cell. The graphite electrode was thus at the bottom of the cell (a scheme is available in the [Supplementary Information](#)). The experiments were performed with 4 ml of solution above the electrode. Some graphite electrodes were coated with poly(3,4-ethylenedioxythiophene) (pedot) by chemical vapour deposition as described in detail elsewhere [29].

Electrochemical measurements were performed with a Biologic VSP2 multi-channel potentiostat. The Nernst potential of the electrode was measured as a function of the current intensity that was passed through it. Current intensities of 1, 20, 50, 100, 150, 200, 250, 300, 350, 400, and finally 150 mA again, were successively imposed through the electrode for 1 min at each value, by using the potentiostat in galvanostatic mode. One Pt wire was connected to the working electrode pin of the potentiostat and the other to the auxiliary electrode pin. A saturated calomel electrode (SCE, 0.24 V vs. the standard hydrogen electrode) was connected to the reference electrode pin. The potential values were measured between the working electrode and the reference electrode pins.

Measurements were repeated around one hour apart. In between, the resistance of the electrode was measured by applying the same series of current intensity values but connecting the reference pin of the potentiostat with the auxiliary electrode pin. In this way, measurement of the working electrode potential gave the cell voltage related to each value of the applied current intensity.

3. Electrochemical basics

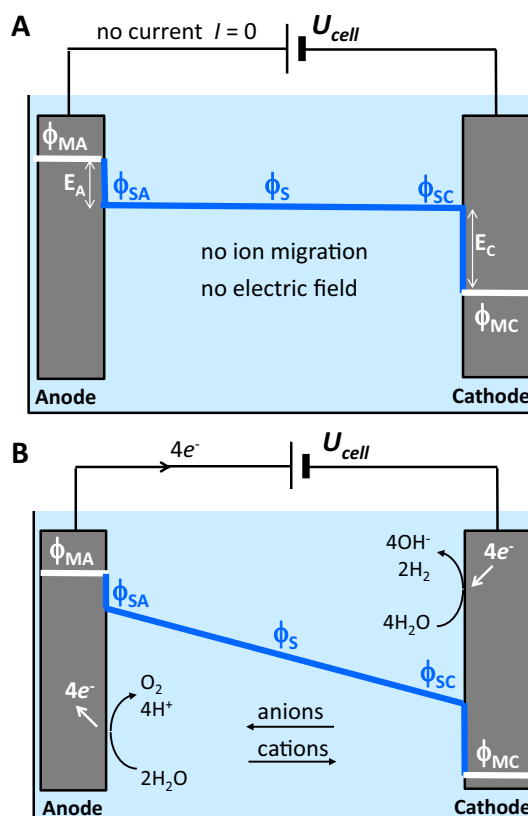
An electrochemical system is commonly described as two electrodes separated by a solution ([Schematic 1](#)). Each point of the system is characterized by the local value of the electrostatic potential ϕ . The electrostatic potential is defined in relation to the amount of work (W) that would be necessary to move a charge (q) from a point at infinity, away from any electrostatic interaction, to the specific point in the material or solution considered, so $W = q\phi$. It is generally assumed that the potential is uniform inside the electrode materials (ϕ_M). This is particularly true for analytical set-ups, because they commonly use small-scaled highly conductive electrodes. At the electrode/solution interfaces, the difference between the electrostatic potential of the electrode material (ϕ_M) and the electrostatic potential of the solution in contact with the electrode surface (ϕ_S) is defined as the Nernst potential (E):

$$E = \phi_M - \phi_S \quad (1)$$

which gives at the anode and the cathode, respectively:

$$E_A = \phi_{MA} - \phi_{SA} \text{ and } E_C = \phi_{MC} - \phi_{SC} \quad (2)$$

The Nernst potential is the parameter commonly used by electrochemists under the usual name of “electrode potential”.



Schematic 1. Distribution of the electrostatic potential (ϕ) between two electrodes. A) No current flows through the system; B) U_{cell} is large enough to lead to current generation: water oxidation at the anode and oxygen reduction at the cathode were used to illustrate possible reactions in the case of DES application.

The cell voltage (U_{cell}) is the difference of the electrostatic potentials between electron outlet and electron inlet of the cell. In conventional electrochemical cells, it corresponds to the potential difference measured between the anode and the cathode:

$$U_{cell} = \phi_{MA} - \phi_{MC} \quad (3)$$

It can be developed into:

$$U_{cell} = (\phi_{MA} - \phi_{SA}) + (\phi_{SA} - \phi_{SC}) + (\phi_{SC} - \phi_{MC}) \quad (4)$$

which leads to:

$$U_{cell} = E_A + (\phi_{SA} - \phi_{SC}) - E_C \quad (5)$$

When no current flows through the solution, the electrostatic potential of the solution is uniform ($\phi_{SA} = \phi_{SC}$) and U_{cell} is simply the sum of the two Nernst potentials (Schematic 1.A). Applying U_{cell} affects the ion distribution at the electrode/solution interfaces but does not drive any ion motion through the solution. In this case, no electric field is applied through the solution.

Depending on the value U_{cell} that is applied between the two electrodes, each value of Nernst potential varies independently as:

$$E_A = E_{A,oc} + \eta_A \quad (6)$$

$$E_C = E_{C,oc} + \eta_C \quad (7)$$

where E_{oc} are the Nernst potential values taken when the system is left at open circuit, and η are the overpotentials. The anode and cathode overpotentials vary independently, according to the chemical composition of the solution and the nature of the electrode surfaces. They determine the kinetics of the electrochemical reactions on each electrode.

When η_A is high enough and η_C low enough (η is negative for cathodic reaction) to generate electrochemical reactions at the electrode surfaces, a current I passes through the system (Schematic 1.B). The current is transported through the solution by the motion of the charged species: the anions towards the anode, the cations towards the cathode. This ion motion is driven by the charge unbalances created at the electrode surfaces: an excess of positively charged species at the anode and the opposite at the cathode. Obviously, electrons are exchanged at exactly the same rate at the anode and cathode surfaces because there is no electron accumulation or depletion in the electrical circuit. Similarly, a reaction can occur at one electrode surface only when the opposite electron exchange occurs at the surface of the other electrode, in order to keep the charge balance in the solution.

When a current flows through the system, the electrostatic potential gradient created in the solution ($\phi_{SA} - \phi_{SC}$), also called the ohmic drop, depends on the ionic resistance of the solution (R_S), according to Ohm's law applied to electrolytes:

$$\phi_{SA} - \phi_{SC} = R_S I \quad (8)$$

The electrostatic potential gradient results in an electric field. Considering two plane electrodes set face to face and separated by a length l , the electric field (\vec{E} , expressed in $V \cdot m^{-1}$) is:

$$\vec{E} = \frac{\phi_{SA} - \phi_{SC}}{l} = \frac{R_S I}{l} \quad (9)$$

The value of the solution resistance is given by:

$$R_S = \rho \frac{l}{A} \quad (10)$$

where $\rho(\Omega m)$ is the ionic resistivity of the solution, and A (m^2) is the cross-sectional area of the solution through which ions flow. The value of the electric field is thus:

$$\vec{E} = \rho \frac{I}{A} \quad (11)$$

Actually, it may be difficult to assess the value of the cross-sectional area (A) of the solution through which ions flow. In the case of two identical plane electrodes face to face, A can be assumed equal to the electrode surface area. Real cases may differ from this scheme when the electrode areas are smaller than the cross-sectional area of the solution. Accurate mapping of the local electric field then requires the current distribution to be solved based on the Poisson equation [30]. Eq. (11) gives an accurate value of the electric field when the cross-sectional area, A , of the solution is known, for instance, when the solution is bounded by insulating walls, for instance, in a closed channel. The equation allows estimations to be made for small analytical devices by using the surface area of the electrodes as the values of A .

It is sometimes useful to introduce the ionic conductivity (σ , $S m^{-1}$ or $\Omega^{-1} m^{-1}$):

$$\sigma = \frac{1}{\rho} \quad (12)$$

because σ can be measured easily. σ can also be evaluated theoretically, when the composition of the solution is known, by using the molar ionic conductivities λ_i ($m^2 S mol^{-1}$), which are available in the literature [31]:

$$\sigma = \sum_i \lambda_i C_i \quad (13)$$

where C_i ($mol m^{-3}$) is the concentration of each charged species.

4. Theoretical analysis of the systems used to apply direct electrical stimuli (DES)

4.1. Zero electrode: Electroless cell culture on conductive supports

The objective of this "zero electrode" sub-section is to briefly recall the considerable impact that the conductive properties of the support can have on cell growth, even in the absence of any electrical stimuli. In some cases, the conductive capability of the support is necessary, even without any external electric stimuli, to achieve optimal cellular function [32]. The term "electroless" is used here by analogy with the conventional electroless process of metal plating, which does not require a current to pass through the support [33,34].

4.1.1. Zero electrode: Short overview

One difficulty in analysing the impact of DES is to distinguish the direct effect of DES from the effect of the conductive support itself. For instance, Ning and co-workers noted recently that, when used as a substrate, conductive polymers encouraged cell proliferation and extension even if no additional electric current was provided [4].

Conductive supports are mainly used in the context of tissue engineering. Many cells cultured on conductive surfaces have a tendency to form 3-dimensional tissues, which is a promising way to design organoids [35-37]. Conductive polymers hold a hegemonic position in tissue engineering [4,38-40] because of their great capacity to favour cell growth and, in some cases, to drive cell differentiation to the formation of a specific tissue.

The suitability of conductive supports for cell proliferation and differentiation can be explained in different ways. Several purely physical and chemical effects have been shown, which are linked to various parameters involved in polymer conductivity, such as surface charge [41]; presence of specific components in the polymeric matrix, counter-ions for instance [42]; enhanced adsorption of proteins [43] and hydrophilic/hydrophobic characteristics. Conductivity of the support has also been assumed to help cells to

communicate with each other by creating new conducting channels [39].

Conductive polymers seem particularly suitable for cardiomyocyte cultivation and cardiac tissue engineering because of their ability to mimic *in vivo* conditions for heart functions [44,45]. Osteogenesis has also been shown to be favoured on conductive supports. For example, the polymer conductivity has been demonstrated to affect calcium deposition into the extracellular matrix of rat bone marrow stroma cells [46]. Fibres of conductive polymers have also proved able to modulate the induction of myoblasts in myotube formation [47].

4.1.2. Zero electrode: Suggestions from the electrochemical standpoint

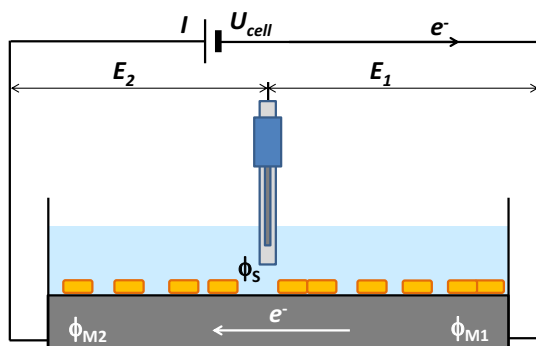
Considering the great impact that the conducting properties of the support can have on cell behaviour, systematically performing control experiments in parallel with the experiments under DES is strongly recommended. The control experiments should obviously use the same support without applying DES. When designing the control experiments, care should also be taken, particularly when using a conductive polymer coating, to avoid possible modification of the support by the DES. Applying a DES may affect the structure, the redox state and the surface properties of the electrode itself [48,49]. The DES may thus impact the cell behaviour by varying the properties of the support. To detect such a possible indirect effect, control experiments in the absence of DES should use supports in both the initial and final states. This means that control experiments must be performed with supports that, respectively, have not / have previously been exposed to the DES in the cell-free culture medium before being exposed to the cells.

4.2. Single electrode

A great number of studies devoted to DES implement experimental devices equipped with a single electrode, through which the current passes. The adherent cells are grown directly on the electrode surface and their behaviour is studied with respect to the current intensity that is imposed through the electrode, or the voltage (U_{cell}) that is applied between the electrode ends (Schematic 2).

A glance at Table 1 shows that this kind of system is mainly used with conductive polymers, which are often incorporated into composite polymers in order to optimize the conductivity, biocompatibility and mechanical properties of the support material.

Applying DES with such a system has been shown to impact cell migration, adhesion, growth, morphology, metabolism and differentiation in different ways. DES can enhance adsorption of extracellular matrix proteins, often fibronectin, on the electrode surface [58,63,64], thus favouring cell adhesion as reviewed in



Schematic 2. Single-electrode experimental device. A complete scheme with the potential profiles is available in Supplementary Information.

[4]. In some cases the DES affects the redox state of the adsorbed proteins and thus disturbs the redox state of cells [65].

Applying a constant potential can modify the electrode oxidation state. For instance, when polypyrrole (PPy) is used, switching from an oxidized state to the neutral state affects the cell culture because of differences in the physicochemical properties of the two polymer redox states: different adsorption of proteins and DNA, different wettability, different surface topography, different surface charge, etc. [48]. DES may also act on cell behaviour by releasing some ions from the polymer matrix [58,66].

DES can drastically modify the local composition of the culture medium. Consumption of oxygen by reduction at the cathode can lead to local harmful anoxic conditions [67,68]. DES can result in the production of some species by the electrochemical reactions [68]. In particular, oxygen reduction is known to produce oxygen reactive species, which can induce cell stress and impact cell proliferation, differentiation [69] and migration [70].

DES can act through more sophisticated ways related to the cell metabolism. Intimate mechanisms have been identified that directly affect certain cellular functions. For example, DES can induce changes in the intracellular calcium concentration by acting on voltage-gated ion channels [71] or by other mechanisms [72]. The impact of DES on interfacial conditions has also been speculated to possibly alter the cell redox homeostasis, which could affect the mitochondrial machinery and subsequently alter the cell metabolic activity [73].

4.2.1. Single electrode: Theoretical analysis

Single electrode systems are highly unusual in the field of electrochemistry and electro-analysis. Generally, in most electrochemical systems, the current flows through the solution via ion transport between the anode and the cathode. Here, on the contrary, the current mainstream flows from one end of the electrode to the other, parallel to the electrode surface, and there is no defined anode and cathode (Schematic 2). In the absence of defined anode and cathode, the cell voltage (U_{cell}) is expressed according to its most general definition, i.e. as the difference of the electrostatic potential between electron outlet and electron inlet of the electrochemical cell. Eq. (3) is thus adapted by replacing the anode and cathode electrostatic potentials (ϕ_{MA} and ϕ_{MC}) by the potentials at the two ends of the device (ϕ_{M2} and ϕ_{M1}):

$$U_{\text{cell}} = \phi_{M2} - \phi_{M1} \quad (14)$$

The solution composition being assumed uniform along the electrode surface, the electrostatic potential of the solution close to the electrode surface (ϕ_S) is uniform. Eq. (4) thus becomes:

$$U_{\text{cell}} = (\phi_{M2} - \phi_S) + (\phi_S - \phi_{M1}) \quad (15)$$

and, according to the definition of the Nernst potential (Eq. (1)):

$$U_{\text{cell}} = E_2 - E_1 \quad (16)$$

The cell voltage induces a gradient of Nernst potential along the electrode. When the applied cell voltage is low, the difference of the Nernst potential between the two electrode ends remains small. In this case, no electrochemical reaction occurs on the electrode. Actually, the charge unbalance that would be created by an electrochemical reaction could not be compensated by an opposite one occurring on the same surface (see section 3). When the difference of the Nernst potentials of the two electrode ends is small, the electrode cannot simultaneously support a reduction and an oxidation reaction on its surface.

It is important to note that the absence of electrochemical reaction means that there is no electron transfer at the electrode/solution interface. There is consequently no electric current passing through the solution, so that there is no electric field through the solution. When the difference of the Nernst potentials of the two

Table 1

Single-electrode devices for application of direct electrical stimuli (DES) on cell cultures. When indicated, l is the length of electrode that the current flows through. BDNF: brain derived neurotrophic factor; MWCNT: multiwalled carbon nanotubes; NGF: Nerve growth factor; PANi: polyaniline; PANi/CPSA/PLCL: polyaniline doped with camphorsulfonic acid, blended with poly(L-lactide-co- ϵ - caprolactone); PCL: polycaprolactone; PDLA: poly-D,L-lactide; PDLA/CL: poly(D,L-lactide-co- ϵ -caprolactone); PDLLA: poly(D,L-lactic acid); PLGA: poly(lactic acid-co-glycolic acid); PLLA : poly L-lactide; PPy: polypyrrole.

Electrode	Cells	Electrical stimuli	DES effect	Ref
<i>L.H. Dao group</i> PPy and PDLA/CL composite	PC12	0, 5, 20 and 50 μ A for 7 days $l = 2.5$ cm	Higher % of neurite under moderate current intensity	[49]
<i>Z. Luo group</i> PPy/chitosan	Schwann cells	100 mV/mm for 4 h	Enhanced expression and secretion of NGF and BDNF	[50]
<i>P. X. Ma group</i> PPy/PDLLA	PC12	100 mV for 2 h	Increased % of neurite-bearing cells and of neurite length	[51]
<i>S. Ramakrishna group</i> PANi/PLLA nanofibres scaffold	Rat nerve stem cells	1.5 V for 1 h $l = 1.5$ cm	Extended neurite outgrowth	[52]
PANi/poly(ϵ -caprolactone)/gelatin	Nerve stem cells	1.5 V for 15, 30 and 60 min	Improved cell proliferation, higher neurite length	[53]
<i>E.C. Schmidt group</i> PPy and PEDOT derivatives	Human mesenchymal stem cell	4 periods, each 10 mV/mm for 8 h + no DES for 40 h	Enhanced differentiation to osteogenesis	[54]
Macroporous PPy/PCL	Glial cells from the peripheral nervous system	50 mV/mm for 1 h $l = 4$ cm	Production of NGF more than tripled	[55]
PPy-coated PLGA NGF-immobilized	PC12	10 mV/cm for 2 h	Improved neurite development	[56]
PPy/poly(lactic-co-glycolic acid) nanofibre scaffold	PC12	100 mV/mm for 2 h	Longer neurites and more neurite formation	[57]
PPy	PC12	10 μ A for 2 h $l = 4$ cm	Enhanced neurite extension	[58]
<i>H. Shin group</i> PANi/CPSA/PLCL nanofibres	Human dermal NIH-3 T3 fibroblasts	Current of 0 to 200 mA for 2 days	Increased mitochondria activity at 20 mA	[59]
<i>J. Weng group</i> PDLA/MWCNT nanofibres	Osteoblasts	50, 100 and 200 μ A 4 h/day for 6 days	Cells grew along the electrical current direction	[60]
<i>Z. Zhang group</i> PPy/PLLA	Human skin fibroblasts	2 V for 1, 2, 4 or 24 h; $l = 2$ cm	Cell viability increased up to 4.0-fold	[61]
PPy/PLLA	Human skin fibroblasts	1 V for 24 h $l = 2$ cm	Enhanced cytokine secretion by 10-fold	[25]
PPy/PLLA	Human skin fibroblasts	Current of 0 to 800 mA for 4 days $l = 2.5$ cm	Higher number of viable cells with medium currents	[62]

electrode ends is small, the current passes entirely through the electrode material and does not create an electric field in solution.

The current that passes along the electrode induces a gradient of Nernst potential (Eq. (16)). Physically, a difference of the Nernst potential reflects a difference in the interfacial environment on the electrode surface. The interfacial environment is thus different between the two ends of the electrode. For instance, if the electrode material locally gets a higher electron density, some cations will come from the solution to the electrode surface or some anions will move away from the electrode surface to compensate the local charge. This may also affect the adsorption/desorption equilibrium of charged species. It must be noted that this charge re-balancing of the interface involves only a minute quantity of ions and in a transient way, just at the moment when the current is switched on. It then results in a stable distribution of the interfacial ionic environment, as long as the current is constant.

Cells growing on the surface of such a single-electrode system consequently find a gradient of the interfacial environment depending on the current that passes through the system. This is certainly the way in which the cells sense the current flowing inside the electrode material. This can impact their adhesion, proliferation, differentiation and metabolic expression as observed in many studies (Table 1), for instance by affecting their membrane potential and the ion fluxes through ion channels. Moreover, the gradient of the interfacial environment between the two electrical connections of the electrode can explain the orientation of cells along the electrical current [60].

This kind of electrochemical device is far from being common in conventional electrochemistry, so an abiotic experiment is presented here to illustrate the dependence of the average Nernst potential of a single-electrode on the current applied through it.

Various values of current intensity were applied through a graphite electrode and its Nernst potential (E_2) was measured with respect to a reference electrode located over it. Fig. 1 shows that the Nernst potential significantly deviated from the open circuit value. It varied almost proportionally to the intensity, by around 15 mV per 100 mA. The presence of a pedot coating did not change the trend.

The maximum current intensities applied in this illustration (400 mA), corresponded to cell voltages, which remained small, about 125 and 100 mV for the pure graphite and the coated graphite electrodes, respectively (resistances were 0.31 and 0.25 Ω , respectively). As the connections were around 17 mm apart, this should correspond to potential gradients of less than 8 mV/mm. In many cases, significantly higher potential gradient or cell voltages are reported in the literature (Table 1). A cell voltage of the order of 2 V is commonly applied between the two ends of the electrode (Eq. 14). Keeping the hypothesis of ϕ_s uniformity, Eq. (16) indicates that the difference of the Nernst potential at the two ends of the electrode can also be evaluated in the 2 V range, i.e., a range where electrochemical reactions may occur. In this case, the part of the electrode upstream of the electron flow ($\phi_{M,1}$) acts as a cathode and the part downstream ($\phi_{M,2}$) as an anode (Schematic 3).

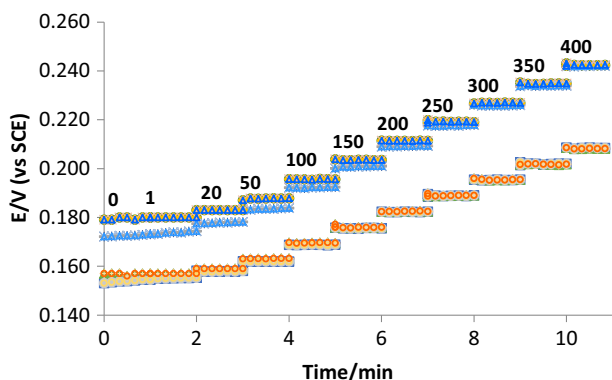
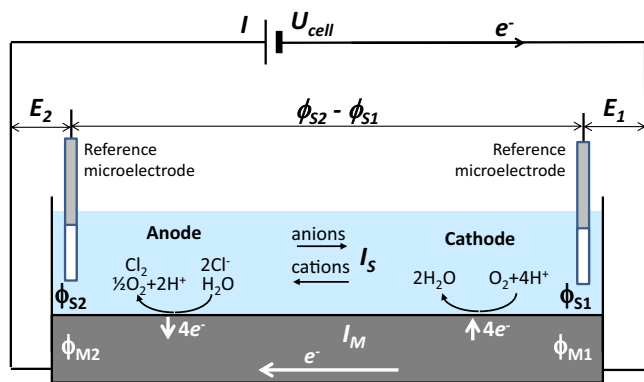


Fig. 1. Potential of single electrode vs. saturated calomel reference (SCE) as a function of time when current intensities of 1 to 400 mA were imposed through it. Electrodes were in graphite (blue triangles; replicates) and graphite coated with pedot (orange circles; replicates). The values of current intensity are indicated in mA on the diagram. (For interpretation of the references to colour in this figure legend, the reader is referred to the web version of this article.)



Schematic 3. Single-electrode device under high cell voltage. The gradient of the electrostatic potential of the electrode material ϕ_M ($\phi_{M1} < \phi_{M2}$) can drive cathodic reactions upstream of the electron flow and anodic ones downstream. Oxygen reduction at the cathode site and water and chloride oxidation at the anode site were chosen as an illustration. The total current (I) applied to the system is divided into the current that passes through the electrode material (I_M) and the current transported through the solution by ion motion (I_S) with $I_S \ll I_M$.

A potential difference of the order 2 V can be sufficient to drive an oxidation reaction at one end and a reduction reaction at the other. For instance, in an aerobic medium, water oxidation at the anode and oxygen reduction at the cathode can be considered as the reverse reactions of the same thermodynamic equilibrium:



In this case, there is no thermodynamic threshold to overcome. U_{cell} applied to the electrode ends should only provide the overpotentials necessary to drive the reactions (combining Eqs. (6) and (7), in which $E_{A,oc} = E_{C,oc}$, and Eq. (16) results in $U_{\text{cell}} = \eta_A + |\eta_C|$).

In an anaerobic environment, considering water oxidation at the anode and water reduction at the cathode, the thermodynamic threshold to be overcome is 1.23 V, so water electrolysis may be possible with U_{cell} of the order of 2 V. The occurrence of electrochemical reactions are even more likely as the conductive materials used for cell culture most often involve very electro-active coatings, including graphene-based material, [74,75] carbon nanotubes [76], and conductive fillers such as carbon black and metallic particles [40]. Such compounds tend to reduce the overpotential necessary to drive many electrochemical reactions.

Such a situation may, to some extent, be similar to that of corrosion, where local anode and cathode sites occur on the same material coupon. In the context of corrosion, the cause is not the application of a potential difference through the material but the local breakdown of the passive layer (pitting corrosion) or the difference in local oxygen concentration (crevice corrosion) for example.

It should be kept in mind that high electrochemical reaction rates are not needed here to disturb the cell environment. Very low currents may be sufficient to modify the local surface conditions (ion composition, production of toxic species, redox state of surface compounds, etc.) in different ways on the anode and cathode sites.

The possible occurrence of anode and cathode sites may affect cell behaviour in various ways. Firstly, as explained in section 3, the local charge unbalances created at the reactive sites lead to the motion of cations towards the cathode and anions towards the anode, i.e. an electric field is created in the solution between the anode and cathode sides. In this case, the electric field can be a supplementary process by which DES affects the cells.

The production and consumption of chemical species can be other important events affecting the cells (see the introduction of section 4.2 above). At the cathode site, the most likely reaction is oxygen reduction. Oxygen reduction is known to produce oxygen reactive species (superoxide ion, hydrogen peroxide, hydroxide ion), which can disturb cell adhesion and proliferation. Chemical stress by oxygen reactive species has also been observed to drive specific differentiation [69] and the oxygen reduction reaction provokes a local pH increase.

At the anode side, water oxidation occurs, except if redox compounds that are more easily oxidized than water are present in the medium. Water oxidation produces oxygen and induces local acidification of the medium. Local oxygen and pH gradients along the electrode can thus result from the occurrence of anode and cathode sides. When chlorides are contained in the medium, they can be oxidized into chlorine, which could drastically affect cell growth.

The electrochemical reactions may involve the electrode material itself, particularly when conductive polymers are used [48]. A decrease of the electrode conductivity has, for instance, been explained by the modification of the polymer structure during application of DES over a long duration [49,62]. Such a reaction may also release ions into the medium.

Here, we can only draw attention to the possibility of the occurrence of cathode and anode sites on single electrodes operating under a significant cell voltage. However, it remains difficult to identify the actual occurrence of such a situation by analysing the experimental data reported in the literature so far, in particular because the Nernst potential of the electrode is never reported, to the best of our knowledge. Experimental work will be necessary to identify whether or not this situation occurs on single electrodes due to the application of DES.

A glance at Table 1 is enough to note that three different parameters are used to characterize the stimuli: the current intensity, the cell voltage or the voltage gradient (i.e. the voltage divided by the length of the electrochemical cell), and that these parameters can have very different values. Generally, the value of only one parameter is given and it is not possible to deduce the others. If the resistance of the electrode (R) was known, current intensity and cell voltage could be easily linked by Ohm's law:

$$U_{\text{cell}} = R I \quad (18)$$

but the value of R is rarely given.

A great number of the studies employing single-electrode devices use various types of conductive polymers, which are generally implemented in the form of thin electrode coatings. These coatings have a large range of electrical conductivity values. For

instance, polypyrrole films exhibit conductivities from 10 to more than 5000 S cm⁻¹ and polyaniline from 30 to 200 S cm⁻¹ [40]. Reported values for the conductivities of the coatings used in single-electrode systems span several orders of magnitude: 10⁻³ S cm⁻¹ [61], 0.0138 S cm⁻¹ [59], 10 S cm⁻¹ [77]. Other reports tend to give the electrode resistance instead, which confirms a wide range of values from a few kΩ to several hundreds of kΩ [54,55,58]. In this context, the single electrode could be addressed as a composite material with two parallel resistances, one for the supporting electrode ($R_{support}$) and one for the coating ($R_{coating}$), which gives:

$$\frac{1}{R} = \frac{1}{R_{support}} + \frac{1}{R_{coating}} \quad (19)$$

This simple equation shows that the link between U_{cell} and the current intensity depends not only on the characteristics of the coating but also on that of the support electrode beneath. Unfortunately, in the literature, no mention is generally made of the characteristic of the support electrode. The same voltage applied through support electrodes of different materials or with different thicknesses can result in different Nernst potentials even when the same coating is used.

The reality of single-electrode devices may be even more complex. The Nernst potential is the difference between the electrostatic potentials of the electrode material (ϕ_M) and the solution close to the electrode surface (ϕ_S) (Eq. (1)). The potential ϕ_M is measured at the electrical connection and it is generally assumed that ϕ_M is uniform from the connecting wire to the surface of the electrode in contact with the solution. This hypothesis remains valid here when the coating is conductive and the contact of the coating with the support electrode is of good electrical quality. Actually, the potential difference of two conductive materials put in contact (called Galvani potential) is generally neglected in the usual context of electrochemistry.

However, this assumption may not be true, depending on the nature of the coating and the quality of the electrical contact between coating and support, particularly when the coating has low conductivity. The electrostatic potential of the coating may then be significantly different from that of the support electrode. Furthermore, the situation can differ depending on whether the electrical connections are made from underneath via the support electrode or are applied directly onto the coating surface. Finally, the electrical behaviour of the electrode can even be more complex if the coating has semi-conductive properties. In conclusion, the same applied current or cell voltage can lead to different Nernst potential gradients depending on various experimental parameters: the nature of the coating, obviously, but also the deposition process and the configuration of the experimental set-up. The relation between the applied current or cell voltage and the resulting Nernst potential can be very different from one system to another and establishing it requires in-depth electrochemical characterization of the devices.

4.2.2. Single electrode: Suggestions from electrochemical standpoint

The current that passes through the electrode modifies the interfacial electrostatic conditions and the electrostatic status of the interface is globally monitored by the value of the Nernst potential. The main advice that can be given here is thus to systematically measure the Nernst potential of the electrode and to use the Nernst potential to discuss the results.

The simplest way to measure the Nernst potential of a single electrode is to place a reference electrode in the solution over the electrode surface and measure the potential difference between one of the electrical connections (e.g. ϕ_{M1}) and the reference electrode (ϕ_S) with a high input impedance voltmeter (Sche-

matic 2). This measure gives one value of the Nernst potential (E_1). The second value (E_2) can be measured by connecting the voltmeter to the other electrical connection of the cell (ϕ_{M2}). It can also be calculated according to Eq. (16). This equation is valid in any case, provided that care is taken not to move the reference electrode from one measurement to the next in order to keep the (ϕ_S) value constant (see Eq. (15)).

Obviously, measuring the Nernst potentials is only a first step. Advancing in deciphering the mechanisms of DES action would then require accurate characterization of the modifications that the current induces in the ionic environment at the interface, by chemical analysis of the interface for instance.

To the best of our knowledge, the occurrence of oxidation and reduction reactions at the surface of such single-electrode setups has never been considered so far, while, as developed above, these reactions can impact cell behaviour in various unanticipated ways. Consequently, carefully checking such systems in abiotic conditions before using them for cell growth or tissue engineering should be seen as a priority.

In this objective, reference micro-electrodes should be used to detect and measure the possible gradient of electrostatic potential in the solution (Schematic 3). Each reference micro-electrode must be placed as close as possible to each end of the electrode and the potential difference between them ($\Delta\phi_S = \phi_{S2} - \phi_{S1}$) measured with a high input impedance voltmeter.

Ag/AgCl microelectrodes can be used, for example, as done to characterize two-electrode systems implemented in microfluidic devices [78,79]. Such pseudo-reference microelectrodes are thin silver wires coated with a silver chloride deposit. A mandatory preliminary check must verify that the potential difference between the two micro-electrodes is zero when no current is flowing through the electrode. Platinum micro-wires can also be used [7] instead of Ag/AgCl microelectrodes. In this case the preliminary check is even more important because the potential of Pt wires is neither stable nor well-defined.

Two cases can occur. If $\Delta\phi_S$ is nil, the electrostatic potential of the solution is uniform. There are no anode and cathode sites on the electrode surface, no current flows through the solution and no electric field is established in solution.

If $\Delta\phi_S$ has a significant value, anode and cathode sites occur at the electrode surface, current flows through the solution and an electric field is established. Most likely, only a small part of the current flowing through the system is diverted into the solution (I_S on Schematic 3), while the vast majority passes right through the electrode material (I_M on Schematic 3), because the current flowing through the solution is limited the rate of the electrochemical reactions at the anode and cathode sites.

It should consequently be recalled here that using the value of the potential difference applied at the electrode ends (U_{cell}) divided by the length of the cell migration zone (l) in order to assess the electric field applied to the cells would give a considerably overestimated value. Actually, most reports indicate only this $\frac{U_{cell}}{l}$ ratio, which gives the false impression that the behaviour of the cells is induced by much stronger electric fields than those that could possibly apply in the solution. Cell growth and differentiation, and tissue development, may consequently be sensitive to considerably lower electric fields than the value of $\frac{U_{cell}}{l}$ has suggested so far. The literature on this topic would certainly benefit from being reviewed after the actual electric field values have been characterized on such systems in the most commonly used configurations.

The electric field in solution can be assessed using Eq. (9) where ($\phi_{SA} - \phi_{SC}$) is ($\phi_{S2} - \phi_{S1}$), combined with Eq. (10) to estimate R_S . Nevertheless, Eq. (10) requires knowledge of the value of the cross-sectional area of the solution through which the current flows. This parameter may be difficult to assess, depending on the experimen-

stal set-up. A minimum value of the electric field can be estimated by using the value of the total cross-section of the solution in Eq. (10).

Actually, the distribution of the electric field in solution can depend on the local distribution of current inside the electrode material, particularly when the electric wires are connected to the support electrode at spots with very small areas and if the electrode material is not highly conductive. An accurate definition of the local electric field values could be obtained by numerical modelling of the electrostatic potential distribution in solution [30].

Finally, it can be noted that, when a reference microelectrode is placed close to each of the ends of the electrode, it is possible to measure the E_1 and E_2 values of the Nernst potential by measuring the potential difference between each reference and the closest electrode end (Schematic 3). These two values will comply with Eq. (16) in the case where the potential of the solution is uniform, i.e. $\Delta \phi_S$ is nil, or will not comply when $\Delta \phi_S$ is not nil. This can be another way to detect the occurrence of anode and cathode sites that induce current in solution.

It must be kept in mind that such an Ag/AgCl electrode, made of an Ag wire coated with an AgCl deposit, immersed in the solution medium can be considered as a pseudo-reference but is not so stable and reliable as a conventional reference electrode. In particular, its potential depends on the chloride concentration of the solution, according to the equation:

$$E_{\text{Ag/AgCl}} = 0.22 - \frac{RT}{F} \ln\left(\frac{[\text{Cl}^-]}{C_0}\right) \quad (20)$$

where $E_{\text{Ag/AgCl}}$ is the potential of the Ag/AgCl electrode vs SHE, R is the gas constant, T is the temperature, F is the Faraday constant,

$[\text{Cl}^-]$ is the chloride concentration and C_0 is the standard concentration equal to 1 M. For example, this equation shows that the potential of a conventional Ag/AgCl reference electrode, equipped with an internal solution of 1 M KCl, is 0.22 V/SHE, while a simple Ag wire coated with AgCl and immersed in a solution that contains 10 mM chloride is 0.34 V/SHE. When the objective is to measure a Nernst potential, the Ag/AgCl wire must consequently be calibrated with respect to a certified Ag/AgCl reference electrode, or any type of reference electrode, in order to know the Nernst potential values vs. a certified reference.

Knowing the values of E_1 and E_2 is essential to decipher what reactions may occur on the electrode surface. Additional abiotic experiments should then be performed to characterize the reactivity of the electrode in the medium. Recording current-voltage curves by low scan voltammetry using a three-electrode system (see section 4.4) should be very useful to define what reactions can occur in the region of the E_1 and E_2 potentials.

4.3. Two-electrode systems (Tables 2, 3 and 4)

Two-electrode devices are mainly used to investigate cell electrotaxis, also sometimes called cell galvanotaxis, i.e. the capacity of cells to orient themselves and migrate in an electric field [80,81]. This is another very large research field with foreseen applications, particularly for tissue repair and wound healing.

The occurrence of a wound in living organisms generates a local electric field, which guides cells to migrate towards the wound and thus favours healing. Applying DES *in vitro* is consequently a common way to mimic the endogenous electric phenomena that occur around wounds [11,13,82,83]. For example, DES has been seen as a

Table 2

Conventional, macro-sized, two-electrode devices for application of direct electrical stimuli (DES) to cell cultures. SS is stainless steel.

Electrode	Cells	Electrical stimuli	DES effect	Ref
<i>E.C. Butcher group</i> Pt electrodes on either side of a Transwell filter	Human peripheral blood lymphocytes	2.5 V for 1.5 h	Motion towards cathode; activates intracellular kinase signalling pathways	[87]
<i>W. Korohoda group</i> Ag/AgCl electrodes Salt bridges	Rat prostate cancer cells	10 to 400 mV/mm for 6 h	Only metastatic cells moved to the cathode	[85]
<i>N.D. Leipzig group</i> Pt electrodes	Human neural stem progenitor cell	0.5 or 1.8 mV/mm 10 min/day for 2 days $i = 0.04$ or 0.14 mA	Longer neurites and signs of differentiation	[90]
<i>S.K. Mallapragada group</i> Ag/AgCl electrodes Salt bridges	Hippocampal neural progenitor cells	437 mV/mm for 16 to 24 h/day for several days $i = 3.4$ mA	Cells aligned perpendicular to the electric field; enhanced differentiation to neurons	[91]
<i>X.-T. Meng group</i> Ag/AgCl electrodes Salt bridges	Neural progenitor cells	50 to 250 mV/mm for 2 or 12 h/day for several days	Higher neuronal differentiation rate	[92]
<i>F.B. Printz group</i> Pt electrodes Salt bridges	Murine adipose-derived stroma cells	100 600 and 1000 mV/mm for 6 h	Dose-dependent migration to the cathode	[96]
<i>Q. Wan group</i> Ag/AgCl electrodes Salt bridges	Neuronal stem/progenitor cells	30 to 250 mV/mm for 3 to 10 h	Migration towards the cathode; novel signal transduction pathway	[97]
<i>L. Yao group</i> Ag/AgCl electrodes Salt bridges	Embryonic stem cells	50 and 100 mV/mm for 20 h	Migration to the cathode enhanced with increased field	[98]
<i>M. Zhao and C.D. McCaig groups</i> Ag/AgCl electrodes Salt bridges	Bovine corneal epithelial cells	0 to 250 mV/mm for 5 h	Migration towards the cathode	[95]
Ag/AgCl electrodes	Hippocampal neurons	120 mV/mm	Migration towards the cathode with small DES	[89]
Ag/AgCl electrodes Salt bridges	Hippocampal cells	50 to 300 mV/mm for 1 h	Affects the axis of cell division and neuronal polarity	[93]
Ag/AgCl electrodes Salt bridges	Retinal pigment epithelial cells	50 to 600 mV/mm for 2 or 5 h	Voltage-dependent migration to the anode	[99]
Ag/AgCl electrodes Salt bridges	Human neural stem cell	16 to 300 mV/mm for 10 to 160 min	Migration to the cathode depended on field strength and time	[84]

Table 3

Two-electrode devices designed in micro-fluidic systems for application of direct electrical stimuli (DES) to cell cultures. The cell migration zone is most often composed of a channel, of length L , width w , and height h .

Electrode - Channel	Cells	Electrical stimuli	Electric field effect	Ref
<i>E.C. Butcher group</i> Pt electrodes 0.25 mm diameter $L = 1.5$ cm, $w = 500$ μ m $h = 100$ μ m	Human peripheral blood lymphocytes	100 mV/mm for 1.5 h $i \approx 2$ μ A	Motion towards cathode; activates intracellular kinase signalling pathways	[87]
<i>M. Yang group</i> Pt electrodes Salt bridges $L = 12$ mm, 3 w values of 100, 150 and 300 μ m, $h = 30$ μ m	Human lung cancer cells H1975	$U_{cell} = 9$ V 150, 300 and 450 mV/mm $I =$ a few μ A (n.c.)	Motion towards cathode; different migration ability correlated to cell characteristics	[103]
Pt electrodes Salt bridges $w = 18$ mm, $h = 465$ μ m	Human lung cancer cells H460, HCC827, H1299, H1975	$U_{cell} = 8.1, 15.6, 22$ V 200, 400, 600 mV/mm $i = 2.8, 5.6, 8.4$ mA	Motion towards cathode or anode depending on cell line; Ca^{2+} signalling involved	[88]
<i>T. Pan group</i> Ag/AgCl electrodes Salt bridges	Human corneal epithelial cell	2.1 mV/mm to 1.6 V/mm	Field-dependent orientation; migration to the cathode	[104]
<i>C.-W. Huang and J.-Y. Cheng group</i> Ag/AgCl electrodes Salt bridges $L = 24$ mm, 3 w values of 5, 1.7 and 1 mm	Human lung cancer cells CL1-5, CL1-0	$U_{cell} = 4$ and 20 V 75 and 375 mV/mm $i = 30$ and 150 μ A for 2 h	Only highly metastatic cells (CL1-5) migrated to the cathode	[7]
Ag/AgCl electrodes Salt bridges $L = 75$ mm, $w = 24$ mm $h = 70$ μ m	Human lung cancer cells CL1-5	$U_{cell} = 21$ V 300 mV/mm for 2 h $i = 696$ mA	Regulation of gene expression involved electrotaxis	[94]
Ag/AgCl electrodes Salt bridges Various lengths of a few centimetres	Oral squamous cancer cell	Different field strengths 300 mV/mm for 2 h $i = 116$ μ A	Migration towards the cathode	[79]
Ag/AgCl electrodes Salt bridges $L = 45$ mm, $w = 3$ mm	Human lung cancer cells CL1-5, CL1-0	300 mV/mm for 2 h	Investigation of signalling pathway	[78]
<i>Y.-S. Sun and J.-Y. Cheng group</i> Ag anode and AgCl cathode; salt bridges Various values of L , $w = 1$ mm, $h = 0.22$ mm	Lung cancer cells	26 to 254 mV/mm fixed by the value of L for 2 h $i = 0.157$ mA	Acts by increasing the production of reactive O_2 species	[102]
Ag anode and AgCl cathode; salt bridges 3.2 mm ² cross-section	NIH 3 T3 fibroblasts	≈ 150 mV/mm $i = 1.3$ mA	Increased healing rate; combined effect of medium composition	[83]
Ag anode and AgCl cathode; salt bridges 3D scaffold included	Lung cancer cells CL1-0, CL1-5, A549	$U_{cell} = 80$ V 290–338 mV/mm $i = 6$ mA	The 3-D scaffold affects cell migration direction and speed	[86]

possible tool to guide neural stem cells towards injured sites of the central nervous system [84]. Electrotaxis may also have applications in cancer research. For example, rat prostate cancer cells have been shown to migrate towards the cathode, or not, depending on their metastatic status [85]. Lung cancer cells have been observed to migrate towards the cathode or the anode depending on the cell line [86]. A brief survey by Lin and co-workers [87] found that some cells migrate towards the cathode (e.g. neural crest cells, fibroblasts, keratinocytes, rat prostate cancer cells, mouse neutrophils, human myeloid cell lines, and many epithelial cell types), and others to the anode (e.g. corneal endothelial cells, and human vascular endothelial cells).

The effect of the electric field on cell motion does not act only through simple electrophoretic migration; it can also impact intracellular mechanisms involved in cell motion [16,78,87-89]. In addition, the electric field can also affect essential cellular functions linked with cell growth [90], cell differentiation [90-93] and gene expression [94].

In electrotaxis studies, the main concern is to generate a clean electric field excluding all the other possible side-phenomena mentioned above (pH gradient, oxygen consumption, release of compounds produced at the electrode, etc.). For instance, the production of reactive oxygen species at the cathode has been described to enhance cell migration [70].

In order to really focus on the effect of the electric field alone, most of the two-electrode devices used in this framework are designed with salt bridges, which separate the medium that contains the cells from the two compartments that contain the electrodes. In this way, the medium containing the cells exchanges only ions with the solution that composes the salt bridges and is protected from the perturbations due to the electrochemical reactions at the electrode surfaces [95]. Macro-sized devices were first designed according to this general principle. Then, similar, smaller configurations, of millimetre sizes, were combined with the amazing potential of microfluidics platforms, bringing a real revival to the topic. In between, a few non-conventional systems consisting of a non-closed electrochemical loop were proposed. These three categories are successively analysed below.

4.3.1. Conventional, macro-sized, two-electrode systems: Theoretical analysis (Table 2)

Macro-sized two-electrode systems are often built in Petri dishes including centimetre-sized cell migration zones [95,100,101]. Unfortunately, macro-sized systems have rarely been described in detail from the electrochemical standpoint. The values of the electric field (\vec{E} , mV·mm⁻¹) are always indicated but little is explained about the way they are applied and calculated. Experimental measurement of the electric field has rarely been reported

for macro-sized devices, although it has been advised for a long time in some reports that describe the experimental protocol in detail [101]. It is possible that electric fields may sometimes have been calculated by dividing the applied U_{cell} by the length of the cell migration zone l (Schematic 4).

First of all, it should be recalled that, when U_{cell} is not high enough, the values of the Nernst potentials are not high enough to drive electrochemical reactions at the electrode surfaces (see section 3, Schematic 1.A). For instance, in an anaerobic solution that does not contain any redox compounds, no reaction can occur for U_{cell} values less than the thermodynamic potential difference of 1.23 V, which is required for water to oxidize at the anode and reduce at the cathode. In this case, no current flows through the solution. The whole potential difference is due to Nernst potentials at the electrode/solution interfaces (Schematic 1.A). The electrostatic potential of the solution is uniform ($\phi_{SA} = \phi_{SC}$) and, according to Eq. (9), no electric field is applied through the solution.

In the context of DES application, it is important to keep in mind that applying a voltage between two electrodes is not sufficient to ensure an electric field through the solution in between. When no current flows through the solution, no electric field occurs. In this case, estimating a non-existent electric field by the $\frac{U_{cell}}{l}$ value would lead to irrelevant discussion. Nevertheless, applying U_{cell} in a range of values that do not produce current impacts the charge status of the interface. It may thus affect the cells growing on the electrode surface, if the set-up does not include a salt bridge.

The voltage, U_{cell} , applied to a two-electrode system can be decomposed according to the different segments that compose the electrochemical loop as schematized in Schematic 4:

$$U_{cell} = (\phi_{MA} - \phi_1) + (\phi_1 - \phi_2) + (\phi_2 - \phi_3) + (\phi_3 - \phi_4) + (\phi_4 - \phi_{SA}) + (\phi_{SA} - \phi_{SC}) + (\phi_{SC} - \phi_5) + (\phi_5 - \phi_6) + (\phi_6 - \phi_7) + (\phi_7 - \phi_8) + (\phi_8 - \phi_{MC}) \quad (21)$$

This sum includes Nernst potentials ($(\phi_{MA} - \phi_1)$ and $(\phi_8 - \phi_{MC})$), junction potentials due to the connections between the solutions and the salt bridges ($(\phi_2 - \phi_3)$, $(\phi_4 - \phi_{SA})$, $(\phi_{SC} - \phi_5)$ and $(\phi_6 - \phi_7)$) and ohmic drops in the electrode compartments ($(\phi_1 - \phi_2)$ and $(\phi_7 - \phi_8)$) and in the salt bridges ($(\phi_3 - \phi_4)$ and $(\phi_5 - \phi_6)$). An elementary evaluation of the electric field applied in the cell migration zone ($\phi_{SA} - \phi_{SC}$) can be made by neglecting the contributions of the Nernst potentials, the junction potentials and the ohmic drops in the electrode compartments, i.e. only taking the ohmic drops along the salt bridges ($(\phi_3 - \phi_4)$ and $(\phi_5 - \phi_6)$) into account, which are most likely to make the greatest contributions because of the length of these elements.

The resistivity, ρ , of the solutions used in cell electrotaxis studies commonly ranges around $0.7 \Omega\text{m}$ [7,91,102]. The cell migration zone is often a rectangular channel 22 mm in length (L) with a

cross-sectional area around 5 mm^2 (10 mm wide and 0.5 mm high) [100,101]. Each salt bridge is generally at least 15 cm long, and is made with tube of 7 mm^2 cross-sectional area [100]. On this basis, the resistances calculated with Eq. (10) are of the order of $3 \text{ } 100 \Omega$ for the cell migration channel and $30 \text{ } 000 \Omega$ for the two salt bridges. If a current of 0.1 mA passes through the system, the value of U_{cell} can be estimated at 3.31 V. If the $\frac{U_{cell}}{l}$ ratio were used to assess the electric field, it would be concluded that a field of 150 mV/mm was applied to the cells. This value considerably overestimates the actual field strength, which is, according to Eq. (11), 14 mV/mm . This example shows how using the ratio $\frac{U_{cell}}{l}$ can lead to a considerable overestimation of the field applied in the cell migration zone.

Such overestimation may have been common in the reports dealing with macro-sized devices including long salt bridges to separate the electrode from the cell migration zone. One of the rare studies that implemented electrodes directly in the cell migration zone [90] dealt with electric fields two orders of magnitude lower than the others (Table 2). So cells may be more sensitive to electric fields than indicated by studies carried out in macro-sized devices.

4.3.2. Micro-fluidic two-electrode systems: Theoretical analysis (Table 3)

The picture is quite different in the case of micro-devices. As recently reviewed [81], cell electrotaxis research has greatly benefited from the development of microfluidic systems, which, in theory, provide cells with a stable, well-controlled micro-environment (pH, temperature, medium composition including nutrients, stimuli, etc.). In this context, the electric field strength is most often calculated with respect to the current intensity that passes through the system according to Eq. (11) [7,86,88,103]. The potential gradient at the extremities of the cell migration channels ($\phi_{SA} - \phi_{SC}$), or even along the cell migration channels, is often checked experimentally by inserting platinum wires [7] or Ag/AgCl wire electrodes [78,79]. The potential distribution has often been modelled numerically [7,78,79,86,88,103] and the theoretical values successfully compared with experimental measurements (Fig. 2).

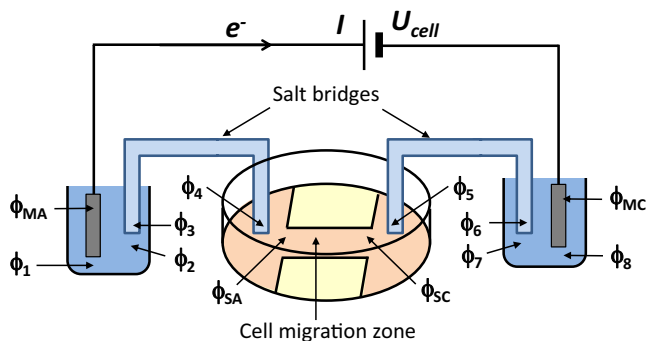
According to Eq. (11), the field strength is inversely proportional to the cross-sectional area of the migration channel. This property has been used in microfluidic devices, by designing channels with different widths in order to obtain different field strengths in exactly the same environment (Fig. 2).

Similarly, according to Eq. (11), the field strength is proportional to the current that passes through the channel. Following this principle, micro-devices have been designed where the ionic current is divided into several pathways in order to obtain different values of the electric field in the same device (Schematic 5). In particular, it is thus possible to achieve the control experiment, i.e. without applied electric field, in the same microfluidic platform.

A glance at Tables 2 and 3 shows that the devices used for electrotaxis experiments are dominated by the use of Ag/AgCl electrodes. It has sometimes been claimed that Ag/AgCl electrodes should be used instead of platinum electrodes to prevent pH changes during long-duration voltage application [79,83]. Actually, at platinum electrodes, reduction of water or of oxygen at the cathode leads to solution alkalization, while oxidation of water at the anode leads to acidification. In contrast, a silver electrode coated with silver chloride deposit achieves the redox reaction:



which does not disturb the solution pH. The concern about pH variation is minor in macro-sized systems, as the electrode compartments are separated from the cell migration zone by long salt bridges, each generally said to be at least 15 cm long. It could be more disturbing in small and micro-systems. The possible distur-



Schematic 4. The two-electrode system used for cell electrotaxis studies, redrawn from [101]. The system is based on a Petri dish with an electrode compartment on each side, ionically connected with a salt bridge.

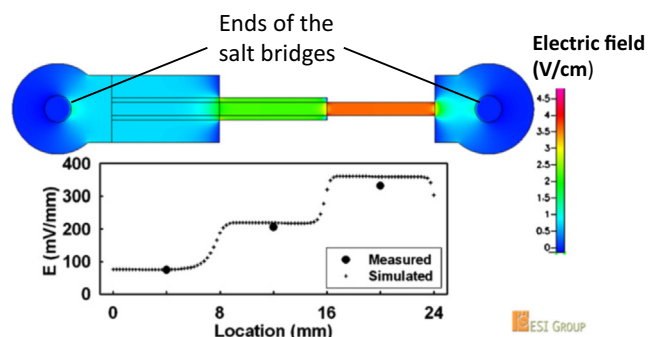
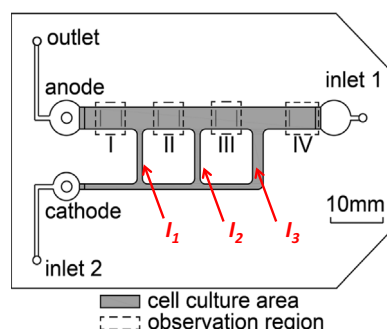


Fig. 2. Top view of the microfluidic channel designed by Huang et al. [7]. The total length of the cell migration channel was 24 mm and it had three different widths: 5, 1.7 and 1 mm. According to Eq. (11), the electric field values were inversely proportional to the channel width, and were measured at 74, 205 and 331 mV/mm in each segment. Numerical modelling of the local electric field was consistent with local measurements.



Schematic 5. Top view of the microfluidic device designed by Tsai et al. [79]. The current flows from the anode to the cathode by different pathways: $I_1 + I_2 + I_3$ flows through zone I, $I_2 + I_3$ flows through zone II, I_3 flows through zone III, while no current flows in zone IV, so the electric field in each segment I to IV has the values 300, 104, 38 and 0 mV/mm, inversely proportional to the current intensity that passes through.

bance of pH has been quantified in a recent article as a function of the charge transferred through the system [105]. The same article also gives helpful information on avoiding possible detrimental transport of Ag^+ ions to the migration zone.

Using Ag/AgCl electrodes may be justified for another reason. Reaction (22) is fast and does not require high overpotentials (Eqs. (6) and (7)) to produce significant current intensity. This is not the case of platinum electrodes, which require high overpotentials both for water oxidation and for cathodic reactions, particularly in the solutions near neutral pH used for cell electro taxis. Using Ag/AgCl electrodes may thus be justified in the objective of minimizing the values of the Nernst potentials ($\phi_{\text{MA}} - \phi_1$) and ($\phi_8 - \phi_{\text{MC}}$) in Eq. (21).

It should be noted that an Ag electrode is sometimes used as the anode instead of the Ag/AgCl electrode (Table 3). This is not important when chlorides are present in solution, because Ag is oxidized

into Ag^+ ions, which precipitate into AgCl, resulting in reaction (22) again.

Nevertheless, using Ag/AgCl electrodes requires some care because the AgCl deposit is consumed at the cathode (Reaction 22). For long-duration experiments, the AgCl deposit could be fully consumed and the Ag electrode would consequently shift to oxygen or water reduction. Such a reaction change could considerably change the value of the current intensity produced when the experiment is based on the application of a constant value of U_{cell} , as is generally the case.

4.3.3. Non-conventional, open-loop, two-electrode devices: Theoretical analysis (Table 4)

This research area has given rise to some experimental devices that are surprising for a conventional electrochemist because they are based on an open electrochemical loop (Table 4). The results provided seem interesting but their interpretation should deserve some care.

One of these non-conventional systems was composed of two electrodes connected electrically and placed in two different wells [106] (Schematic 6.A). There was no ionic bridge between the two wells, which were fully independent. There was consequently no ionic connection between the two electrodes. A power generator was assumed to apply potential differences from 0 to 500 mV between the two electrodes. No current can flow through the electrodes in such a system, and this was definitely the objective of the authors: to apply a high cell voltage in the absence of current. Experimentally, current of the order of 100 pA was measured, which was probably a residual current due to a drift of the electronic device.

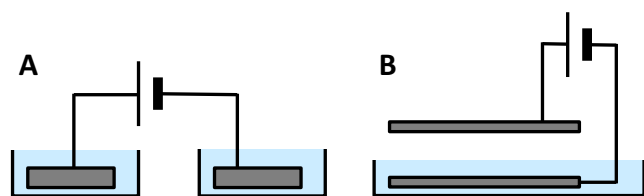
Such a system is surprising from an electrochemical standpoint because it is not possible to apply a controlled value of voltage between two electrodes without any ionic connection in between. The applied voltage may affect the interfacial charge balance at the electrode surfaces, as speculated by the authors, but in a way likely to depend on the electronic circuit of the power generator. It can be speculated that an electron deficit is imposed at the anode, while an electron excess is created at the cathode. This interpretation can explain the effects observed on cell differentiation: the trend towards a negatively (or less positively) charged interface promoted the differentiation of osteoblasts [106].

Nevertheless, it is difficult to establish a link between the electrode status and the voltage value displayed on the apparatus. If such a system did have to be used, it would be helpful to measure the Nernst potential of each electrode, by inserting a reference electrode into each compartment. Obtaining this basic information may be a first step to establishing a possible link between an electrochemical parameter and biochemical observations.

The other non-conventional system had an electrode left in air, without any contact with the solution [107] (Schematic 6.B). Here the presence of an electrode left in air above the solution and its position, whether parallel to the cell migration plane or not, cannot have any influence, contrary to what is suggested in the report. Notably, the presence of the electrode in air does not generate an electric field in the solution.

Table 4
Non-conventional, open-loop, two-electrode devices for application of direct electrical stimuli (DES) on cell cultures. SS: stainless steel.

Electrode	Cells	Electrical stimuli	DES effect	Ref
<i>Z. Schwartz group</i>				
Two titanium electrodes in separate wells without ionic connection	Osteoblasts MG63	Voltage of 0, 100, 200, 300, 400 and 500 mV for 2 h and 22 h	Cathodic polarization decreased cell proliferation and increased production of differentiation markers	[106]
<i>B. Basu group</i>				
Carbon electrode for cell growth and SS electrode above in air	Neuroblastoma cells N2a	0 to 1 V/mm for 6 h	Neurite length depended on field strength	[107]



Schematic 6. Non-conventional systems. A. No ionic connection between the anode and cathode wells; B. One electrode left in air.

To conclude on this sub-section, it is advisable that such non-conventional experimental devices be avoided and the effect of the interfacial state of the electrode surface be studied with a suitable analytical device and protocol, notably using three-electrode systems.

4.3.4. Two electrode-systems: Suggestions from the electrochemical standpoint

The lack of experimental details in many of the reports devoted to macro-sized systems may raise concerns that field values have been estimated with the $\frac{U_{cell}}{L}$ ratio. If this is the case, the numerical illustration developed above shows that the field values were considerably overestimated. The response of the cells would therefore have been induced by much weaker fields than assumed. In other words, the cells could be much more sensitive to electric fields than suggested by the experiments carried out in macro-sized systems. It would therefore be advisable to explore the effect of electric fields one order, or even two orders of magnitude smaller than those usually used, i.e. of the order of a few mV/mm. Such a range of values has rarely been investigated so far but some studies have indicated that cells appear to be sensitive to such weak electric fields [90]. This could lead to a whole area of the cell electrotaxis research field being revisited.

One way to measure the electric field really applied to the cells can be to insert a reference microelectrode at each end of the migration zone (as discussed in section 4.2 for single electrodes). Such systems have sometimes been proposed [108,109] but apparently rarely implemented.

Great progress has been achieved in the electrochemical approach to two-electrode systems with the development of micro-fluidic devices. The electric field values have been calculated with respect to the current intensity flowing through the system,

the local distribution of electric field has been modelled numerically, and the theoretical values have been confirmed by experimental measurements in different devices. This approach should be extended to all systems including macro-sized systems.

Nevertheless, even in the context of microfluidic devices, the voltage U_{cell} often seems to be applied instead of the current. Progress still needs to be made in experimental protocols, by systematically applying the current that flows through the system rather than the voltage. Controlling the current allows direct, accurate control of the electric field, according to Eq. (11). In contrast, applying a voltage can result in variable current values and consequently variable electric field values. This can particularly occur in long-term experiments because of possible variation of the electrode characteristics, as detailed above for the Ag/AgCl electrodes that are often used. The same voltage can also result in different values of the current from one experiment to another, depending on the electrode characteristics, and particularly on the electrode surface area.

To sum up, in order to give accurate and stable values of the electric field, experiments should definitively be performed by imposing the current intensity through the system in galvanostatic conditions. The electric field can be measured directly by inserting two reference microelectrodes, each at one end of the migration zone, or it can be calculated according to Eq. (11). A last piece of advice is to take care to measure the ionic resistivity, or ionic conductivity (Eq. 12), at the same temperature as those used for the experiments because temperature can have a significant effect on the value determined [105].

4.4. Three-electrode systems

Three-electrode systems are the most commonly used systems in the field of analytical electrochemistry. A reference electrode is inserted into the current lines, as close as possible to one of the electrodes, which is then called the working electrode. Thanks to a potentiostat, the potential of the working electrode is adjusted to the chosen value, which can be constant or vary as a function of time. In other cases, the current intensity can be imposed and the potentiostat then measures the evolution of the potential of the working electrode as a function of time. Such analytical systems have sometimes been used to study DES effects on cell behaviour, particularly in the field of biomaterial corrosion (Table 5).

Table 5
Three-electrode devices for application of direct electrical stimuli (DES) to cell cultures. PPy: polypyrrole.

Electrode	Cells	Electrical stimuli	DES effect	Ref
J.L. Gilbert group Ti-6Al-4 V alloy	MC3T3-E1 pre-osteoblasts	-0.3 to -0.6 V vs. Ag/AgCl in steps of 50 mV for 24 h	Cell death associated with cathodic current density	[73]
CoCrMo alloy	MC3T3-E1 pre-osteoblasts	-1.0, -0.4 and 0.5 V vs. Ag/AgCl applied for 24 h or less	Cell death at some potentials; changes in cell morphology correlated to current	[68]
Titanium	MC3T3-E1 pre-osteoblasts	-0.4 and -0.5 V vs. Ag/AgCl for 24 h	Anodized surface extended the voltage viability range	[111]
CoCrMo alloy	MC3T3-E1 pre-osteoblasts		Cell death outside a voltage viability range	[65]
R. Langer group Fibronectin-coated PPy (oxidized)	Bovine aortic endothelial cells	-0.25 V vs Ag/AgCl	Inhibited cell extension and DNA synthesis	[48]
ITO			No effect	
E.C. Schmidt group NGF immobilized on PPy	PC12	0.1 V vs Ag pseudo-reference for 2 h and 24 h	50% increase in neurite outgrowth	[77]
PPy film	PC12	0.1 V vs Ag pseudo-reference for 2 h	Increased neurite lengths	[112]
C.H. Thomas group Titanium	Osteoblasts from rat calvarial bone	0 or -1.0 V vs Ag/AgCl for 2 h	Effect of low cathodic potential	[67]

From an electrochemical point of view, this type of system is to be strongly promoted when the objective is to study the effect of the physicochemical status of the electrode interface on the cells that develop on this surface, because it allows the electrochemical state of the electrode to be controlled. When simple basic rules are respected [110], the Nernst potential of the electrode is uniform and the reactions that occur at its surface can be fairly well determined. Actually, the possibility of determining all the reactions that occur at the surface of a well-controlled working electrode depends, to a great extent, on the complexity of the chemical composition of the solution. As cell culture media generally have complex chemical compositions, control experiments in the absence of cells are essential.

Surprisingly, three-electrode systems are still underexploited in the domain of cell research. Apart from very specific cases, we believe that they should be preferred to single-electrode systems, which provide the cells with too many different stimuli on their surface, making it difficult to unravel the tangle of mechanisms.

5. Conclusion

Direct electrical stimuli have been applied to cell cultures by using many different electrochemical systems. These systems have been analysed here through the prism of electrochemical basics.

In the case of single-electrode systems, light was shed on various phenomena that can explain the effect of DES on cell behaviour in different ways. The dependence of the Nernst potential of a single electrode on the current intensity that flows through it has been shown experimentally here. This is unexpected information in the context of conventional electrochemistry, and may afford a way to explain the impact of such single-electrode systems on cells. When the single electrode is resistive, as is the case when conductive polymers are implemented, the reader is made aware of the possible occurrence of anode and cathode sites and of all the consequences that can result.

The two-electrode systems used to study cell electrotaxis should now be implemented and their results discussed in terms of current intensity, rather than voltage, in order to find the correct values of the electric field. The overestimation of electric fields, which can be suspected in many studies, should prompt repeat experiments with much lower values and perhaps lead researchers to reconsider the sensitivity of cells to electric fields. We hope that these theoretical analyses and suggestions, viewed from the electrochemical standpoint, will help the research community to forge ahead in unravelling the complex links between electricity and cell physiology.

Declaration of Competing Interest

The authors declare that they have no known competing financial interests or personal relationships that could have appeared to influence the work reported in this paper.

Acknowledgements

This work is part of the TECH project, entitled "Looking for extracellular electron transfers with human cells" (ANR-17-CE07-45). The authors thank L. Etcheverry and C. Perez (Laboratoire de Génie Chimique) for their useful help with experiments, and B. Caussat, H. Vergnes and M. Mirabedin (Laboratoire de Génie Chimique) for providing pedot-coated graphite electrodes.

Appendix A. Supplementary data

Supplementary data to this article can be found online at <https://doi.org/10.1016/j.bioelechem.2020.107737>.

References

- [1] S. Ingvar, Reaction of cells to the galvanic current in tissue cultures, *Exp. Biol. Med.* 17 (8) (1920) 198–199, <https://doi.org/10.3181/00379727-17-105>.
- [2] G. Marsh, H.W. Beams, In vitro control of growing chick nerve fibers by applied electric currents, *J. Cell. Comp. Physiol.* 27 (3) (1946) 139–157, <https://doi.org/10.1002/jcp.1030270303>.
- [3] C.A.L. Bassett, R.J. Pawluk, R.O. Becker, Effects of Electric Currents on Bone In Vivo, *Nature* 204 (4959) (1964) 652–654, <https://doi.org/10.1038/204652a0>.
- [4] C. Ning, Z. Zhou, G. Tan, Y.e. Zhu, C. Mao, Electroactive polymers for tissue regeneration: Developments and perspectives, *Prog. Polym. Sci.* 81 (2018) 144–162, <https://doi.org/10.1016/j.progpolymsci.2018.01.001>.
- [5] R. Balint, N.J. Cassidy, S.H. Cartmell, Electrical Stimulation: A Novel Tool for Tissue Engineering, *Tissue Eng. Part B: Rev.* 19 (1) (2013) 48–57, <https://doi.org/10.1089/ten.teb.2012.0183>.
- [6] R.H.W. Funk, Endogenous electric fields as guiding cue for cell migration, *Front. Physiol.* 6 (2015), <https://doi.org/10.3389/fphys.2015.00143>.
- [7] C.-W. Huang, J.-Y. Cheng, M.-H. Yen, T.-H. Young, Electrotaxis of lung cancer cells in a multiple-electric-field chip, *Biosens. Bioelectron.* 24 (1) (2009) 3510–3516, <https://doi.org/10.1016/j.bios.2009.05.001>.
- [8] Y. Li, W.-K. Yu, L. Chen, Y.-S. Chan, D. Liu, C.-C. Fong, T. Xu, G. Zhu, D. Sun, M. Yang, Electrotaxis of tumor-initiating cells of H1975 lung adenocarcinoma cells is associated with both activation of stretch-activated cation channels (SACCs) and internal calcium release, *Bioelectrochemistry* 124 (2018) 80–92, <https://doi.org/10.1016/j.bioelechem.2018.03.013>.
- [9] B. Farhoud, R. Nuccitelli, I.R. Schwab, R.R. ISSEROFF, DC Electric Fields Induce Rapid Directional Migration in Cultured Human Corneal Epithelial Cells, *Exp. Eye Res.* 70 (5) (2000) 667–673, <https://doi.org/10.1006/exer.2000.0830>.
- [10] B. Song, M. Zhao, J.V. Forrester, C.D. McCaig, Electrical cues regulate the orientation and frequency of cell division and the rate of wound healing in vivo, *Proc. Natl. Acad. Sci.* 99 (21) (2002) 13577–13582, <https://doi.org/10.1073/pnas.202235299>.
- [11] R. Nuccitelli, A Role for Endogenous Electric Fields in Wound Healing, in: *Curr. Top. Dev. Biol.*, Academic Press, 2003, pp. 1–26, [https://doi.org/10.1016/S0070-2153\(03\)58001-2](https://doi.org/10.1016/S0070-2153(03)58001-2).
- [12] M.E. Mycielska, M.B.A. Djamgoz, Cellular mechanisms of direct-current electric field effects: galvanotaxis and metastatic disease, *J. Cell Sci.* 117 (9) (2004) 1631–1639, <https://doi.org/10.1242/jcs.01125>.
- [13] C.D. McCaig, A.M. Rajniecek, B. Song, M. Zhao, Controlling Cell Behavior Electrically: Current Views and Future Potential, *Physiol. Rev.* 85 (3) (2005) 943–978, <https://doi.org/10.1152/physrev.00020.2004>.
- [14] M. Zhao, Electrical fields in wound healing—An overriding signal that directs cell migration, *Semin. Cell Dev. Biol.* 20 (6) (2009) 674–682, <https://doi.org/10.1016/j.semdb.2008.12.009>.
- [15] E. Wang, M. Zhao, J.V. Forrester, C.D. McCaig, Re-orientation and Faster, Directed Migration of Lens Epithelial Cells in a Physiological Electric Field, *Exp. Eye Res.* 71 (1) (2000) 91–98, <https://doi.org/10.1006/exer.2000.0858>.
- [16] X. Li, J. Kolega, Effects of Direct Current Electric Fields on Cell Migration and Actin Filament Distribution in Bovine Vascular Endothelial Cells, *J. Vasc. Res.* 39 (2002) 391–404, <https://doi.org/10.1159/000064517>.
- [17] E. Wang, M. Zhao, J.V. Forrester, C.D. McCaig, Bi-directional migration of lens epithelial cells in a physiological electrical field, *Exp. Eye Res.* 76 (1) (2003) 29–37, [https://doi.org/10.1016/S0014-4835\(02\)00257-9](https://doi.org/10.1016/S0014-4835(02)00257-9).
- [18] W.S. Beane, J. Morokuma, J.M. Lemire, M. Levin, Bioelectric signaling regulates head and organ size during planarian regeneration, *Development* 140 (2) (2013) 313–322, <https://doi.org/10.1242/dev.086900>.
- [19] V.P. Pai, S. Aw, T. Shomrat, J.M. Lemire, M. Levin, Transmembrane voltage potential controls embryonic eye patterning in *Xenopus laevis*, *Development* 139 (2) (2012) 313–323, <https://doi.org/10.1242/dev.073759>.
- [20] M. Levin, W. Bement, Molecular bioelectricity: how endogenous voltage potentials control cell behavior and instruct pattern regulation in vivo, *MBoC* 25 (24) (2014) 3835–3850, <https://doi.org/10.1091/mbc.e13-12-0708>.
- [21] M. Levin, C.J. Martyniuk, The bioelectric code: An ancient computational medium for dynamic control of growth and form, *Biosystems* 164 (2018) 76–93, <https://doi.org/10.1016/j.biosystems.2017.08.009>.
- [22] B.M. Isaacson, R.D. Bloebaum, Bone bioelectricity: What have we learned in the past 160 years?, *J. Biomed. Mater. Res. 95A* (4) (2010) 1270–1279, <https://doi.org/10.1002/jbm.a.32905>.
- [23] A. Zeighami, F. Alizadeh, M. Saviz, Optimal currents for electrical stimulation of bone fracture repair: A computational analysis including variations in frequency, tissue properties, and fracture morphology: Optimal Currents for Stimulation of Fractures, *Bioelectromagnetics* 40 (2) (2019) 128–135, <https://doi.org/10.1002/bem.22173>.
- [24] A. Majjer, A. Gessner, B. Trumppatori, J.D. Varhus, Bioelectric Dressing Supports Complex Wound Healing in Small Animal Patients, *Top. Companion Anim. Med.* 33 (1) (2018) 21–28, <https://doi.org/10.1053/j.tcam.2018.02.001>.
- [25] G. Shi, Z.e. Zhang, M. Rouabhia, The regulation of cell functions electrically using biodegradable polypyrrole–polylactide conductors, *Biomaterials* 29 (28) (2008) 3792–3798, <https://doi.org/10.1016/j.biomaterials.2008.06.010>.

- [26] Sundelacruz, M. Levin, D.L. Kaplan, Membrane Potential Controls Adipogenic and Osteogenic Differentiation of Mesenchymal Stem Cells, *PLOS ONE*. 3 (2008) e3737. <https://doi.org/10.1371/journal.pone.0003737>.
- [27] I. Titushkin, S. Sun, J. Shin, M. Cho, Physicochemical Control of Adult Stem Cell Differentiation: Shedding Light on Potential Molecular Mechanisms, *J. Biomed. Biotechnol.* 2010 (2010) 1–14, <https://doi.org/10.1155/2010/743476>.
- [28] I. Titushkin, M. Cho, Regulation of Cell Cytoskeleton and Membrane Mechanics by Electric Field: Role of Linker Proteins, *Biophys. J.* 96 (2) (2009) 717–728, <https://doi.org/10.1016/j.bpj.2008.09.035>.
- [29] M. Mirabedin, H. Vergnes, N. Caussé, C. Vahlas, B. Caussat, An out of the box vision over oxidative chemical vapor deposition of PEDOT involving sublimed iron trichloride, *Synth. Met.* 266 (2020) 116419, <https://doi.org/10.1016/j.synthmet.2020.116419>.
- [30] R. Lacroix, S.D. Silva, M.V. Gaig, R. Rousseau, M.-L. Délia, A. Bergel, Modelling potential/current distribution in microbial electrochemical systems shows how the optimal bioanode architecture depends on electrolyte conductivity, *Phys. Chem. Chem. Phys.* 16 (41) (2014) 22892–22902, <https://doi.org/10.1039/C4CP02177K>.
- [31] M. Oliot, S. Galier, H. Roux de Balmain, A. Bergel, Ion transport in microbial fuel cells: Key roles, theory and critical review, *Appl. Energy* 183 (2016) 1682–1704, <https://doi.org/10.1016/j.apenergy.2016.09.043>.
- [32] K. Hosoyama, M. Ahumada, K. Goel, M. Ruel, E.J. Suuronen, E.I. Alarcon, Electroconductive materials as biomimetic platforms for tissue regeneration, *Biotechnol. Adv.* 37 (3) (2019) 444–458, <https://doi.org/10.1016/j.biotechadv.2019.02.011>.
- [33] M.A. Azmah Hanim, 3.15 Electroless Plating as Surface Finishing in Electronic Packaging, in: M. Hashmi (Ed.), *Compr. Mater. Finish.*, Elsevier, Oxford, 2017: pp. 220–229. <https://doi.org/10.1016/B978-0-12-803581-8.09177-3>.
- [34] A.M. Tarditi, M.L. Bosko, L.M. Cornaglia, 3.1 Electroless Plating of Pd Binary and Ternary Alloys and Surface Characteristics for Application in Hydrogen Separation, in: M. Hashmi (Ed.), *Compr. Mater. Finish.*, Elsevier, Oxford, 2017: pp. 1–24. <https://doi.org/10.1016/B978-0-12-803581-8.09166-9>.
- [35] G. Lalwani, S.C. Patel, B. Sitharaman, Two- and Three-Dimensional All-Carbon Nanomaterial Assemblies for Tissue Engineering and Regenerative Medicine, *Ann. Biomed. Eng.* 44 (6) (2016) 2020–2035, <https://doi.org/10.1007/s10439-16-1623-5>.
- [36] T. Lu, Y. Li, T. Chen, Techniques for fabrication and construction of three-dimensional scaffolds for tissue engineering, *Int. J. Nanomedicine*. 8 (2013) 337–350, <https://doi.org/10.2147/IJN.S38635>.
- [37] Z. Zhang, L.H. Klausen, M. Chen, M. Dong, Electroactive Scaffolds for Neurogenesis and Myogenesis: Graphene-Based Nanomaterials, *Small* 14 (48) (2018) 1801983, <https://doi.org/10.1002/sml.201801983>.
- [38] R. Balint, N.J. Cassidy, S.H. Cartmell, Conductive polymers: Towards a smart biomaterial for tissue engineering, *Acta Biomater.* 10 (6) (2014) 2341–2353, <https://doi.org/10.1016/j.actbio.2014.02.015>.
- [39] M. Gajendiran, J. Choi, S.-J. Kim, K. Kim, H. Shin, H.-J. Koo, K. Kim, Conductive biomaterials for tissue engineering applications, *J. Ind. Eng. Chem.* 51 (2017) 12–26, <https://doi.org/10.1016/j.jiec.2017.02.031>.
- [40] G. Kaur, R. Adhikari, P. Cass, M. Bown, P. Gunatillake, Electrically conductive polymers and composites for biomedical applications, *RSC Adv.* 5 (47) (2015) 37553–37567, <https://doi.org/10.1039/C5RA01851J>.
- [41] Z. Zhou, W. Li, T. He, L. Qian, G. Tan, C. Ning, Polarization of an electroactive functional film on titanium for inducing osteogenic differentiation, *Sci Rep* 6 (1) (2016), <https://doi.org/10.1038/srep35512>.
- [42] V. Lundin, A. Herland, M. Berggren, E.W.H. Jager, A.I. Teixeira, Control of Neural Stem Cell Survival by Electroactive Polymer Substrates, *PLOS ONE*. 6 (2011) e18624. <https://doi.org/10.1371/journal.pone.0018624>.
- [43] D.A. Stout, J. Yoo, A.N. Santiago-Miranda, T.J. Webster, Mechanisms of greater cardiomyocyte functions on conductive nanoengineered composites for cardiovascular applications, *Int. J. Nanomedicine*. (2012), <https://doi.org/10.2147/IJN.S34574>.
- [44] Y. Liu, J. Lu, G. Xu, J. Wei, Z. Zhang, X. Li, Tuning the conductivity and inner structure of electrospun fibers to promote cardiomyocyte elongation and synchronous beating, *Mater. Sci. Eng., C* 69 (2016) 865–874, <https://doi.org/10.1016/j.msec.2016.07.069>.
- [45] B.S. Spearman, A.J. Hodge, J.L. Porter, J.G. Hardy, Z.D. Davis, T. Xu, X. Zhang, C. E. Schmidt, M.C. Hamilton, E.A. Lipke, Conductive interpenetrating networks of polypyrrole and polycaprolactone encourage electrophysiological development of cardiac cells, *Acta Biomater.* 28 (2015) 109–120, <https://doi.org/10.1016/j.actbio.2015.09.025>.
- [46] C. Li, Y.-T. Hsu, W.-W. Hu, The Regulation of Osteogenesis Using Electroactive Polypyrrole Films, *Polymers*. 8 (2016) 258. <https://doi.org/10.3390/polym8070258>.
- [47] I. Jun, S. Jeong, H. Shin, The stimulation of myoblast differentiation by electrically conductive sub-micron fibers, *Biomaterials* 30 (11) (2009) 2038–2047, <https://doi.org/10.1016/j.biomaterials.2008.12.063>.
- [48] J.Y. Wong, R. Langer, D.E. Ingber, Electrically conducting polymers can noninvasively control the shape and growth of mammalian cells, *Proc. Natl. Acad. Sci.* 91 (8) (1994) 3201–3204, <https://doi.org/10.1073/pnas.91.8.3201>.
- [49] Z.e. Zhang, M. Rouabhia, Z. Wang, C. Roberge, G. Shi, P. Roche, J. Li, L.H. Dao, Electrically Conductive Biodegradable Polymer Composite for Nerve Regeneration: Electricity-Stimulated Neurite Outgrowth and Axon Regeneration, *Artif. Organs* 31 (1) (2007) 13–22, <https://doi.org/10.1111/j.1525-1594.2007.00335.x>.
- [50] J. Huang, X. Hu, L. Lu, Z. Ye, Q. Zhang, Z. Luo, Electrical regulation of Schwann cells using conductive polypyrrole/chitosan polymers, *J. Biomed. Mater. Res.* 9999A (2009) NA–NA, <https://doi.org/10.1002/jbm.a.32511>.
- [51] H. Xu, J.M. Holzwarth, Y. Yan, P. Xu, H. Zheng, Y. Yin, S. Li, P.X. Ma, Conductive PPY/PDLLA conduit for peripheral nerve regeneration, *Biomaterials* 35 (1) (2014) 225–235, <https://doi.org/10.1016/j.biomaterials.2013.10.002>.
- [52] M.P. Prabhakaran, L. Ghasemi-Mobarakeh, G. Jin, S. Ramakrishna, Electrospun conducting polymer nanofibers and electrical stimulation of nerve stem cells, *J. Biosci. Bioeng.* 112 (5) (2011) 501–507, <https://doi.org/10.1016/j.jbiosc.2011.07.010>.
- [53] L. Ghasemi-Mobarakeh, M.P. Prabhakaran, M. Morshed, M.H. Nasr-Esfahani, S. Ramakrishna, Electrical Stimulation of Nerve Cells Using Conductive Nanofibrous Scaffolds for Nerve Tissue Engineering, *Tissue Eng. Part A* 15 (11) (2009) 3605–3619, <https://doi.org/10.1089/ten.tea.2008.0689>.
- [54] J.G. Hardy, R.C. Sukhvasi, D. Aguilar, M.K. Villancio-Wolter, D.J. Mouser, S.A. Geissler, L. Nguy, J.K. Chow, D.L. Kaplan, C.E. Schmidt, Electrical stimulation of human mesenchymal stem cells on biomineralized conducting polymers enhances their differentiation towards osteogenic outcomes, *J. Mater. Chem. B* 3 (41) (2015) 8059–8064, <https://doi.org/10.1039/C5TB00714C>.
- [55] J.G. Hardy, R.C. Cornelison, R.C. Sukhvasi, R.J. Saballos, P. Vu, D.L. Kaplan, C.E. Schmidt, Electroactive Tissue Scaffolds with Aligned Pores as Instructive Platforms for Biomimetic Tissue Engineering, *Bioengineering*. 2 (2015) 15–34. <https://doi.org/10.3390/bioengineering2010015>.
- [56] J.Y. Lee, C.A. Bashur, C.A. Milroy, L. Forciniti, A.S. Goldstein, C.E. Schmidt, Nerve Growth Factor-Immobilized Electrically Conducting Fibrous Scaffolds for Potential Use in Neural Engineering Applications, *IEEE Trans. Nanobiosci.* 11 (1) (2012) 15–21, <https://doi.org/10.1109/TNB.2011.2159621>.
- [57] J.Y. Lee, C.A. Bashur, A.S. Goldstein, C.E. Schmidt, Polypyrrole-coated electrospun PLGA nanofibers for neural tissue applications, *Biomaterials* 30 (26) (2009) 4325–4335, <https://doi.org/10.1016/j.biomaterials.2009.04.042>.
- [58] A. Kotwal, C.E. Schmidt, Electrical stimulation alters protein adsorption and nerve cell interactions with electrically conducting biomaterials, *Biomaterials* 22 (2001) 1055–1064, [https://doi.org/10.1016/S0142-9612\(00\)00344-6](https://doi.org/10.1016/S0142-9612(00)00344-6).
- [59] S.I. Jeong, I.D. Jun, M.J. Choi, Y.C. Nho, Y.M. Lee, H. Shin, Development of Electroactive and Elastic Nanofibers that contain Polyaniline and Poly(L-lactide-co-ε-caprolactone) for the Control of Cell Adhesion, *Macromol. Biosci.* 8 (7) (2008) 627–637, <https://doi.org/10.1002/mabi.200800005>.
- [60] S. Shao, S. Zhou, L. Li, J. Li, C. Luo, J. Wang, X. Li, J. Weng, Osteoblast function on electrically conductive electrospun PLA/MWCNTs nanofibers, *Biomaterials* 32 (11) (2011) 2821–2833, <https://doi.org/10.1016/j.biomaterials.2011.01.051>.
- [61] G. Shi, M. Rouabhia, S. Meng, Z.e. Zhang, Electrical stimulation enhances viability of human cutaneous fibroblasts on conductive biodegradable substrates, *J. Biomed. Mater. Res.* 84A (4) (2008) 1026–1037, <https://doi.org/10.1002/jbm.a.31337>.
- [62] G. Shi, M. Rouabhia, Z. Wang, L.H. Dao, Z.e. Zhang, A novel electrically conductive and biodegradable composite made of polypyrrole nanoparticles and polylactide, *Biomaterials* 25 (13) (2004) 2477–2488, <https://doi.org/10.1016/j.biomaterials.2003.09.032>.
- [63] Y. Li, K.G. Neoh, E.-T. Kang, Plasma protein adsorption and thrombus formation on surface functionalized polypyrrole with and without electrical stimulation, *J. Colloid Interface Sci.* 275 (2) (2004) 488–495, <https://doi.org/10.1016/j.jcis.2004.02.060>.
- [64] Y. Li, K.G. Neoh, E.T. Kang, Controlled release of heparin from polypyrrole-poly(vinyl alcohol) assembly by electrical stimulation, *J. Biomed. Mater. Res.* 73A (2) (2005) 171–181, <https://doi.org/10.1002/jbm.a.30286>.
- [65] M. Haeri, T. Wöllert, G.M. Langford, J.L. Gilbert, Electrochemical control of cell death by reduction-induced intrinsic apoptosis and oxidation-induced necrosis on CoCrMo alloy in vitro, *Biomaterials* 33 (27) (2012) 6295–6304, <https://doi.org/10.1016/j.biomaterials.2012.05.054>.
- [66] N.K. Guimard, N. Gomez, C.E. Schmidt, Conducting polymers in biomedical engineering, *Prog. Polym. Sci.* 32 (8–9) (2007) 876–921, <https://doi.org/10.1016/j.progpolymsci.2007.05.012>.
- [67] J.L. Gilbert, L. Zarka, E. Chang, C.H. Thomas, The reduction half cell in biomaterials corrosion: Oxygen diffusion profiles near and cell response to polarized titanium surfaces, *J. Biomed. Mater. Res.* 42 (1998) 321–330, [https://doi.org/10.1002/\(SICI\)1097-4636\(199811\)42:2<321::AID-JBM18>3.0.CO;2-L](https://doi.org/10.1002/(SICI)1097-4636(199811)42:2<321::AID-JBM18>3.0.CO;2-L).
- [68] M. Haeri, J.L. Gilbert, Study of cellular dynamics on polarized CoCrMo alloy using time-lapse live-cell imaging, *Acta Biomater.* 9 (11) (2013) 9220–9228, <https://doi.org/10.1016/j.actbio.2013.06.040>.
- [69] E. Serena, E. Figallo, N. Tandon, C. Cannizzaro, S. Gerecht, N. Elvassore, G. Vunjak-Novakovic, Electrical stimulation of human embryonic stem cells: Cardiac differentiation and the generation of reactive oxygen species, *Exp. Cell Res.* 315 (20) (2009) 3611–3619, <https://doi.org/10.1016/j.yexcr.2009.08.015>.
- [70] S.-Y. Wu, H.-S. Hou, Y.-S. Sun, J.-Y. Cheng, K.-Y. Lo, Correlation between cell migration and reactive oxygen species under electric field stimulation, *Biomicrofluidics* 9 (5) (2015) 054120, <https://doi.org/10.1063/1.4932662>.
- [71] J. Zhang, M. Li, E.-T. Kang, K.G. Neoh, Electrical stimulation of adipose-derived mesenchymal stem cells in conductive scaffolds and the roles of voltage-gated ion channels, *Acta Biomater.* 32 (2016) 46–56, <https://doi.org/10.1016/j.actbio.2015.12.024>.
- [72] L. Khatib, D.E. Golan, M. Cho, Physiologic electrical stimulation provokes intracellular calcium increase mediated by phospholipase C activation in

- human osteoblasts, *FASEB j.* 18 (15) (2004) 1903–1905, <https://doi.org/10.1096/fj.04-1814fje>.
- [73] S. Sivan, S. Kaul, J.L. Gilbert, The effect of cathodic electrochemical potential of Ti-6Al-4V on cell viability: voltage threshold and time dependence: The Effect of Cathodic Potential of Ti-6Al-4V on Cells, *J. Biomed. Mater. Res.* 101 (8) (2013) 1489–1497, <https://doi.org/10.1002/jbm.b.32970>.
- [74] Kenry, W.C. Lee, K.P. Loh, C.T. Lim, When stem cells meet graphene: Opportunities and challenges in regenerative medicine, *Biomaterials* 155 (2018) 236–250, <https://doi.org/10.1016/j.biomaterials.2017.10.004>.
- [75] X. Ding, H. Liu, Y. Fan, Graphene-Based Materials in Regenerative Medicine, *Adv. Healthcare Mater.* 4 (10) (2015) 1451–1468, <https://doi.org/10.1002/adhm.201500203>.
- [76] X. Li, X.i. Liu, J. Huang, Y. Fan, F.-Z. Cui, Biomedical investigation of CNT based coatings, *Surf. Coat. Technol.* 206 (4) (2011) 759–766, <https://doi.org/10.1016/j.surfcoat.2011.02.063>.
- [77] N. Gomez, C.E. Schmidt, Nerve growth factor-immobilized polypyrrole: Bioactive electrically conducting polymer for enhanced neurite extension, *J. Biomed. Mater. Res.* 81A (1) (2007) 135–149, <https://doi.org/10.1002/jbm.a.31047>.
- [78] H.-F. Tsai, C.-W. Huang, H.-F. Chang, J.J.W. Chen, C.-H. Lee, J.-Y. Cheng, Evaluation of EGFR and RTK Signaling in the Electrotaxis of Lung Adenocarcinoma Cells under Direct-Current Electric Field Stimulation, *PLoS ONE* 8 (2013). <https://doi.org/10.1371/journal.pone.0073418>.
- [79] H.-F. Tsai, S.-W. Peng, C.-Y. Wu, H.-F. Chang, J.-Y. Cheng, Electrotaxis of oral squamous cell carcinoma cells in a multiple-electric-field chip with uniform flow field, *Biomicrofluidics* 6 (3) (2012) 034116, <https://doi.org/10.1063/1.4749826>.
- [80] B. Cortese, I.E. Palamà, S. D'Amone, G. Gigli, Influence of electrotaxis on cell behaviour, *Integr. Biol.* 6 (9) (2014) 817–830, <https://doi.org/10.1039/C4IB00142G>.
- [81] Y.-S. Sun, Studying Electrotaxis in Microfluidic Devices, *Sensors* 17 (2017). <https://doi.org/10.3390/s17092048>.
- [82] C.D. McCaig, A.M. Rajniecek, B. Song, M. Zhao, Has electrical growth cone guidance found its potential?, *Trends Neurosci.* 25 (7) (2002) 354–359, [https://doi.org/10.1016/S0166-2236\(02\)02174-4](https://doi.org/10.1016/S0166-2236(02)02174-4).
- [83] Y.-S. Sun, S.-W. Peng, J.-Y. Cheng, In vitro electrical-stimulated wound-healing chip for studying electric field-assisted wound-healing process, *Biomicrofluidics* 6 (3) (2012) 034117, <https://doi.org/10.1063/1.4750486>.
- [84] J.-F. Feng, J. Liu, X.-Z. Zhang, L. Zhang, J.-Y. Jiang, J. Nolta, M. Zhao, Guided Migration of Neural Stem Cells Derived from Human Embryonic Stem Cells by an Electric Field, *STEM CELLS* 30 (2) (2012) 349–355, <https://doi.org/10.1002/stem.779>.
- [85] M.B.A. Djamgoz, M. Mycielska, Z. Madeja, S.P. Fraser, W. Korohoda, Directional movement of rat prostate cancer cells in direct-current electric field: involvement of voltage-gated Na⁺ channel activity, *J. Cell Sci.* 114 (2001) 2697–2705 (accessed April 14, 2020) <https://jcs.biologists.org/content/114/14/2697>.
- [86] Y.-S. Sun, S.-W. Peng, K.-H. Lin, J.-Y. Cheng, Electrotaxis of lung cancer cells in ordered three-dimensional scaffolds, *Biomicrofluidics* 6 (1) (2012) 014102, <https://doi.org/10.1063/1.3671399.2>.
- [87] F. Lin, F. Baldessari, C.C. Gyenge, T. Sato, R.D. Chambers, J.G. Santiago, E.C. Butcher, Lymphocyte Electrotaxis In Vitro and In Vivo, *J Immunol* 181 (4) (2008) 2465–2471, <https://doi.org/10.4049/jimmunol.181.4.2465>.
- [88] Y. Li, T. Xu, X. Chen, S. Lin, M. Cho, D. Sun, M. Yang, Effects of direct current electric fields on lung cancer cell electrotaxis in a PMMA-based microfluidic device, *Anal. Bioanal. Chem.* 409 (8) (2017) 2163–2178, <https://doi.org/10.1007/s00216-016-0162-0>.
- [89] L.i. Yao, L. Shanley, C. McCaig, M. Zhao, Small applied electric fields guide migration of hippocampal neurons, *J. Cell. Physiol.* 216 (2) (2008) 527–535, <https://doi.org/10.1002/jcp.21431>.
- [90] L.J. Kobelt, A.E. Wilkinson, A.M. McCormick, R.K. Willits, N.D. Leipzig, Short Duration Electrical Stimulation to Enhance Neurite Outgrowth and Maturation of Adult Neural Stem Progenitor Cells, *Ann. Biomed. Eng.* 42 (10) (2014) 2164–2176, <https://doi.org/10.1007/s10439-014-1058-9>.
- [91] C.A. Ariza, A.T. Fleury, C.J. Tormos, V. Petruk, S. Chawla, J. Oh, D.S. Sakaguchi, S. K. Mallapragada, The Influence of Electric Fields on Hippocampal Neural Progenitor Cells, *Stem Cell Rev. Rep.* 6 (4) (2010) 585–600, <https://doi.org/10.1007/s12015-010-9171-0>.
- [92] Z.-Y. Dong, Z. Pei, Z. Li, Y.-L. Wang, A. Khan, X.-T. Meng, Electric field stimulation induced neuronal differentiation of filum terminale derived neural progenitor cells, *Neurosci. Lett.* 651 (2017) 109–115, <https://doi.org/10.1016/j.neulet.2017.05.001>.
- [93] L.i. Yao, C.D. McCaig, M. Zhao, Electrical signals polarize neuronal organelles, direct neuron migration, and orient cell division, *Hippocampus* 19 (9) (2009) 855–868, <https://doi.org/10.1002/hipo.20569>.
- [94] C.-W. Huang, H.-Y. Chen, M.-H. Yen, J.J.W. Chen, T.-H. Young, J.-Y. Cheng, Gene Expression of Human Lung Cancer Cell Line CL1–5 in Response to a Direct Current Electric Field, *PLoS ONE* 6 (2011). <https://doi.org/10.1371/journal.pone.0025928>.
- [95] M. Zhao, A. Agius-Fernandez, J.V. Forrester, C.D. McCaig, Orientation and directed migration of cultured corneal epithelial cells in small electric fields are serum dependent, *J. Cell Sci.* 109 (1996) 1405–1414 (accessed May 4, 2020) <https://jcs.biologists.org/content/109/6/1405>.
- [96] K.E. Hammerick, M.T. Longaker, F.B. Prinz, In vitro effects of direct current electric fields on adipose-derived stromal cells, *Biochem. Biophys. Res. Commun.* 397 (1) (2010) 12–17, <https://doi.org/10.1016/j.bbrc.2010.05.003>.
- [97] L. Li, Y.H. El-Hayek, B. Liu, Y. Chen, E. Gomez, X. Wu, K.e. Ning, L. Li, N. Chang, L. Zhang, Z. Wang, X. Hu, Q.i. Wan, Direct-Current Electrical Field Guides Neuronal Stem/Progenitor Cell Migration, *Stem Cells* 26 (8) (2008) 2193–2200, <https://doi.org/10.1634/stemcells.2007-1022>.
- [98] Y. Li, M. Weiss, L.i. Yao, Directed Migration of Embryonic Stem Cell-derived Neural Cells In An Applied Electric Field, *Stem Cell Rev. Rep.* 10 (5) (2014) 653–662, <https://doi.org/10.1007/s12015-014-9518-z>.
- [99] O.L. Gamboa, J. Pu, J. Townend, J.V. Forrester, M. Zhao, C. McCaig, N. Lois, Electrical stimulation of retinal pigment epithelial cells, *Exp. Eye Res.* 91 (2) (2010) 195–204, <https://doi.org/10.1016/j.exer.2010.04.018>.
- [100] X. Meng, W. Li, F. Young, R. Gao, L. Chalmers, M. Zhao, B. Song, Electric Field-controlled Directed Migration of Neural Progenitor Cells in 2D and 3D Environments, *J. Vis. Exp. JoVE* (2012). <https://doi.org/10.3791/3453>.
- [101] B. Song, Y. Gu, J. Pu, B. Reid, Z. Zhao, M. Zhao, (21) (PDF) Application of direct current electric fields to cells and tissues in vitro and modulation of wound electric field in vivo, *ResearchGate*. (2007). https://www.researchgate.net/publication/6290532_Application_of_direct_current_electric_fields_to_cells_and_tissues_in_vitro_and_modulation_of_wound_electric_field_in_vivo (accessed April 10, 2020).
- [102] K.-Y. Lo, S.-Y. Wu, Y.-S. Sun, A microfluidic device for studying the production of reactive oxygen species and the migration in lung cancer cells under single or coexisting chemical/electrical stimulation, *Microfluid Nanofluid* 20 (1) (2016). <https://doi.org/10.1007/s10404-015-1683-0>.
- [103] Y. Li, T. Xu, H. Zou, X. Chen, D. Sun, M. Yang, Cell migration microfluidics for electrotaxis-based heterogeneity study of lung cancer cells, *Biosens. Bioelectron.* 89 (2017) 837–845, <https://doi.org/10.1016/j.bios.2016.10.002>.
- [104] S. Zhao, K. Zhu, Y. Zhang, Z. Zhu, Z. Xu, M. Zhao, T. Pan, ElectroTaxis-on-a-Chip (ETC): an integrated quantitative high-throughput screening platform for electrical field-directed cell migration, *Lab Chip* 14 (22) (2014) 4398–4405, <https://doi.org/10.1039/C4LC00745J>.
- [105] A. Schopf, C. Boehler, M. Asplund, Analytical methods to determine electrochemical factors in electrotaxis setups and their implications for experimental design, *Bioelectrochemistry* 109 (2016) 41–48, <https://doi.org/10.1016/j.bioelechem.2015.12.007>.
- [106] R.A. Gittens, R. Olivares-Navarrete, R. Rettew, R.J. Butera, F.M. Alamgir, B.D. Boyan, Z. Schwartz, Electrical polarization of titanium surfaces for the enhancement of osteoblast differentiation: Ti Polarization Enhances OB Differentiation, *Bioelectromagnetics* 34 (8) (2013) 599–612, <https://doi.org/10.1002/bem.21810>.
- [107] S. Jain, A. Sharma, B. Basu, Vertical electric field stimulated neural cell functionality on porous amorphous carbon electrodes, *Biomaterials* 34 (37) (2013) 9252–9263, <https://doi.org/10.1016/j.biomaterials.2013.08.057>.
- [108] W. Korohoda, M. Mycielska, E. Janda, Z. Madeja, Immediate and long-term galvanotactic responses of *Amoeba proteus* to dc electric fields, *Cell Motil.* 45 (2000) 10–26, [https://doi.org/10.1002/\(SICI\)1097-0169\(200001\)45:1<10::AID-CM2>3.0.CO;2-T](https://doi.org/10.1002/(SICI)1097-0169(200001)45:1<10::AID-CM2>3.0.CO;2-T).
- [109] J. Sroka, E. Zimolag, S. Lasota, W. Korohoda, Z. Madeja, Electrotaxis: Cell Directional Movement in Electric Fields, in: A. Gautreau (Ed.), *Cell Migr. Methods Protoc.*, Springer, New York, NY, 2018: pp. 325–340. https://doi.org/10.1007/978-1-4939-7701-7_23.
- [110] M. Rimboud, D. Pocaznoi, B. Erable, A. Bergel, Electroanalysis of microbial anodes for bioelectrochemical systems: basics, progress and perspectives, *Phys. Chem. Chem. Phys.* 16 (31) (2014) 16349–16366, <https://doi.org/10.1039/C4CP01698J>.
- [111] Morteza Haeri, Torsten Wöllert, George M. Langford, Jeremy L. Gilbert, Voltage-controlled cellular viability of preosteoblasts on polarized cpTi with varying surface oxide thickness, *Bioelectrochemistry* 94 (2013) 53–60, <https://doi.org/10.1016/j.bioelechem.2013.06.002>.
- [112] C.E. Schmidt, V.R. Shastri, J.P. Vacanti, R. Langer, Stimulation of neurite outgrowth using an electrically conducting polymer, *Proc. Natl. Acad. Sci.* 94 (17) (1997) 8948–8953, <https://doi.org/10.1073/pnas.94.17.8948>.